MicroRNA miR-24 enhances tumor invasion and metastasis by targeting PTPN9 and PTPRF to promote EGF signaling

William W. Du[1,2,*], Ling Fang[1,2,*], Minhui Li[1,3,2], Xiangling Yang[1,2], Yaoyun Liang[4], Chun Peng[1,4], Wei Qian[5], Yunxia Q. O'Malley[6], Ryan W. Askeland[6], Sonia L. Sugg[6], Jun Qian[5], Jiang Lin[5], Zide Jiang[3], Albert J. Yee[1], Michael Sefton[1], Zhaoqun Deng[1,2], Sze Wan Shan[1,2], Chia-Hui Wang[1,2] and Burton B. Yang[1,2,‡]

[1]Sunnybrook Research Institute, Sunnybrook Health Sciences Centre, Toronto, M4N 3M5, Canada
[2]Department of Laboratory Medicine and Pathobiology, University of Toronto, Toronto, M5S 1A8, Canada
[3]Department of Plant Pathology, South China Agricultural University, Guangzhou, China
[4]Departments of Biology, York University, Toronto, M3J 1P3, Canada
[5]The Affiliated People's Hospital of Jiangsu University, Zhenjiang City, China
[6]Division of Surgical Oncology and Endocrine Surgery, University of Iowa Carver College of Medicine, Iowa City, IA 52242, USA

*These authors contributed equally
‡Author for correspondence (byang@sri.utoronto.ca)

Accepted 24 January 2013
Journal of Cell Science 126, 1440–1453

doi: 10.1242/jcs.118299

Summary

MicroRNAs are known to play regulatory roles in gene expression associated with cancer development. We analyzed levels of the microRNA miR-24 in patients with breast carcinoma and found that miR-24 was higher in breast carcinoma samples than in benign breast tissues. We generated constructs expressing miR-24 and studied its functions using both *in vitro* and *in vivo* techniques. We found that the ectopic expression of miR-24 promoted breast cancer cell invasion and migration. *In vivo* experiments in mice indicated that the expression of miR-24 enhanced tumor growth, invasion into local tissues, metastasis to lung tissues and decreased overall mouse survival. In the miR-24-expressing cells and tumors, EGFR was highly phosphorylated, whereas expression of the phosphatases tyrosine-protein phosphatase non-receptor type 9 (PTPN9) and receptor-type tyrosine-protein phosphatase F (PTPRF) were repressed. We confirmed that miR-24 could directly target both PTPN9 and PTPRF. Consistent with this, we found that the levels of phosphorylated epidermal growth factor receptor (pEGFR) were higher whereas the levels of PTPN9 and PTPRF were lower in the patients with metastatic breast carcinoma. Ectopic expression of PTPN9 and PTPRF decreased pEGFR levels, cell invasion, migration and tumor metastasis. Furthermore, we found that MMP2, MMP11, pErk, and ADAM15 were upregulated, whereas TIMP2 was downregulated; all of which supported the roles of miR-24 in tumor invasion and metastasis. Our results suggest that miR-24 plays a key role in breast cancer invasion and metastasis. miR-24 could potentially be a target for cancer intervention.

Key words: MicroRNA, miR-24, pEGFR, Tumor invasion, Metastasis

Introduction

MicroRNAs (miRNA) are non-coding single-stranded RNA molecules with 18–24 nucleotides, which are produced from endogenous transcripts of short stem-loop structures. Through binding to the 3′-untranslated region (3′UTR) of different target mRNAs (mRNAs), microRNAs can repress the translation of the target mRNAs (Seitz et al., 2003). As a new class of regulatory molecules, miRNAs have diverse functions in cell proliferation (Shatseva et al., 2011; Viticchiè et al., 2011; Yu et al., 2012), survival (Fang et al., 2012a; Ye et al., 2011), invasion (Deng et al., 2011; Luo et al., 2012; Siragam et al., 2012), cell differentiation (Goljanek-Whysall et al., 2012; Kahai et al., 2009; Rutnam and Yang, 2012b), morphogenesis (Wang et al., 2008a), tissue growth (Shan et al., 2009), angiogenesis (Fang et al., 2011; Lee et al., 2007; Smits et al., 2010; Zou et al., 2012), tumor development (Nohata et al., 2012; Volinia et al., 2006) and metastasis (Huang et al., 2008; Ma et al., 2007; Rutnam and Yang, 2012a). The largest functional group of miRNAs is the one involved in cancer development. Recent studies have shown that miR-24 can inhibit apoptosis of both cancer cells (Qin et al., 2010) and cardiomyocytes (Qian et al., 2011) and can accelerate cell proliferation (Zaidi et al., 2009). Upregulation of miR-24 has been observed in oral carcinoma (Lin et al., 2010) and is one of the most abundant miRNAs in cervical cancer (Wang et al., 2008b). It appears that miR-24 can repress expression of the tumor suppressor $p16^{INK4a}$ (Lal et al., 2008). Overall however, the role of miR-24 in cancer cell invasion and metastasis is still not clear.

Epidermal growth factor receptor (EGFR) is a member of the receptor tyrosine kinases. It is expressed on the cell surface mediating a variety of signals associated with cell proliferation. It has been demonstrated that altered expression of EGFR could result in cancer development (Zhang et al., 2007). Furthermore, breast cancer patients with EGFR upregulation have a less favorable prognosis than those with EGFR-negative tumors (Koletsa et al., 2010). Phosphorylation of EGFR plays a crucial role in the biological functions of EGFR (Magkou et al., 2008). Protein-tyrosine phosphatases can remove the phosphate groups

Journal of Cell Science

from the phosphorylated receptor tyrosine kinases (Tonks, 2006) and antagonize their activity (Zhu et al., 2008). It has been reported that tyrosine-protein phosphatase non-receptor type 9 (PTPN9) can dephosphorylate EGFR and inhibit growth and invasion of MBA-MD-231 cells (Yuan et al., 2010). The role of other PTPs in EGFR dephosphorylation is not clear. In this study, we demonstrated that miR-24 can activate EGFR phosphorylation resulting in enhanced tumor growth, tumor local invasion and metastasis, which resulted in decreased animal survival. Consistent with this was the activation of EGFR. The activation of EGFR activity was achieved by repressing expression of two phosphatases PTPN9 and receptor-type tyrosine-protein phosphatase F (PTPRF). We confirmed that both PTPN9 and PTPRF were the targets of miR-24.

Results

Increased expression of miR-24 in human breast carcinoma

To dissect the roles of miRNA in breast cancer development, we examined miRNA levels in breast cancer tissues and normal breast tissues. RNAs isolated from the paraffin-embedded tissues were subjected to real-time PCR analysis. The assays showed that miR-24 levels were significantly higher in breast tumor tissue than in the corresponding normal breast tissue from the same patient (Fig. 1A, $P=0.000136$). We also isolated RNAs from frozen tumor tissues and the surrounding normal breast tissues. Real-time PCR analysis indicated that of the 23 pair specimens obtained from 23 patients, 15 pairs of samples showed higher levels of miR-24 in the tumors than in the normal tissues, while the other eight pairs showed lower levels of miR-24 in the tumor tissues (Fig. 1B). These experiments suggested that miR-24 may play a role in cancer development.

miR-24 promoted cell invasion, migration, proliferation and cell-cell interaction

We generated a miR-24 expression construct (Fig. 1C) which was transfected into breast cancer cells, and then used cell sorting to isolate a stable pooled cell line. After confirming integration of the construct into the genome (supplementary material Fig. S1A, upper) and expression of miR-24 (supplementary material Fig. S1A, lower), we conducted cell invasion assays. Mock- and miR-24-transfected 4T1 cells were loaded onto a Transwell insert with serum-free Dulbecco's modified Eagle's medium (DMEM) and then incubated at 37℃ for 24 hours. The invasive cells were stained and counted in six randomly selected fields under a light

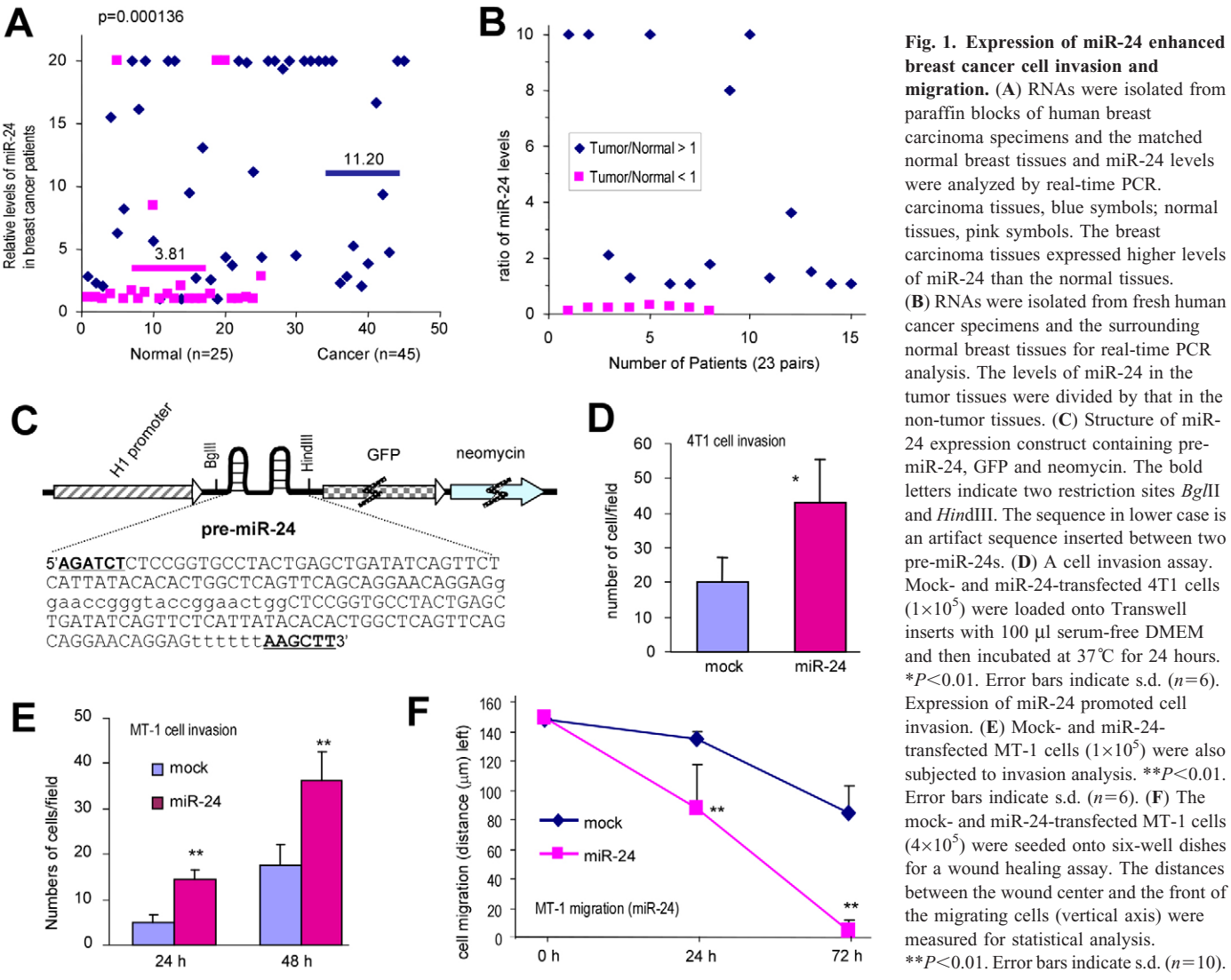

Fig. 1. Expression of miR-24 enhanced breast cancer cell invasion and migration. (**A**) RNAs were isolated from paraffin blocks of human breast carcinoma specimens and the matched normal breast tissues and miR-24 levels were analyzed by real-time PCR. carcinoma tissues, blue symbols; normal tissues, pink symbols. The breast carcinoma tissues expressed higher levels of miR-24 than the normal tissues. (**B**) RNAs were isolated from fresh human cancer specimens and the surrounding normal breast tissues for real-time PCR analysis. The levels of miR-24 in the tumor tissues were divided by that in the non-tumor tissues. (**C**) Structure of miR-24 expression construct containing pre-miR-24, GFP and neomycin. The bold letters indicate two restriction sites *Bgl*II and *Hin*dIII. The sequence in lower case is an artifact sequence inserted between two pre-miR-24s. (**D**) A cell invasion assay. Mock- and miR-24-transfected 4T1 cells (1×10^5) were loaded onto Transwell inserts with 100 μl serum-free DMEM and then incubated at 37℃ for 24 hours. $^*P<0.01$. Error bars indicate s.d. ($n=6$). Expression of miR-24 promoted cell invasion. (**E**) Mock- and miR-24-transfected MT-1 cells (1×10^5) were also subjected to invasion analysis. $^{**}P<0.01$. Error bars indicate s.d. ($n=6$). (**F**) The mock- and miR-24-transfected MT-1 cells (4×10^5) were seeded onto six-well dishes for a wound healing assay. The distances between the wound center and the front of the migrating cells (vertical axis) were measured for statistical analysis. $^{**}P<0.01$. Error bars indicate s.d. ($n=10$).

microscope. We found that cells transfected with miR-24 displayed higher levels of invasion than the mock-transfected cells (Fig. 1D; supplementary material Fig. S1B). To corroborate this result, we performed the invasion assay in a human breast cancer cell line MT-1 (Fig. 1E; supplementary material Fig. S1C) and found that expression of miR-24 promoted cancer cell invasion. The invasion assay was also performed in the presence of Matrigel and we confirmed that 4T1 cells transfected with miR-24 had higher invasive capacity than the mock-transfected cells (supplementary material Fig. S1D).

Cell migration assays were performed to examine the role of miR-24. Mock- and miR-24-transfected 4T1 and MT-1 cells were cultured until 95% confluence. The monolayer of cells was wounded and the cultures were maintained in the presence of mytomycin to inhibit cell proliferation. Cell migration was photographed under a light microscope every 24 hours. The distances between the wounding center and the front of the migrating cells were measured for statistical analysis. The experiments indicated that expression of miR-24 promoted migration of MT-1 cells (Fig. 1F; supplementary material Fig. S1E) and 4T1 cells (supplementary material Fig. S1F).

We examined proliferation of 4T1 cells transfected with miR-24 or the control vector. The experiments showed that the miR-24-transfected cells had higher rates of proliferation than the vector-transfected cells (supplementary material Fig. S1G). Analysis of cell cycle progression indicated that more vector-transfected cells than miR-24-transfected cells were in the G1 phase suggesting a lower rate of proliferation of the former cells (supplementary material Fig. S1H). Consistent with this was the finding that miR-24-transfected cells formed more and larger colonies than the mock-transfected cells in the colony formation assays (supplementary material Fig. S2A). In sphere formation assays, we observed that the miR-24-transfected cells formed more and large spheres than the mock-transfected cells (supplementary material Fig. S2B). In low serum conditions, the miR-24-transfected cells showed increased adhesion and spreading relative to the mock-transfected cells (supplementary material Fig. S2C). The above characteristics of the miR-24-transfected cells were indicative of metastatic cancer cells. We thus performed drug-resistance experiments by culturing the mock- and miR-24-transfected MT-1 cells in the presence of Docetaxel, Doxorubicin and Epirubicin and found that the miR-24-transfected cells were more resistant to these drugs than the mock-transfected cells (supplementary material Fig. S2D).

To corroborate the role of miR-24 in mediating cell activities, we developed an antisense construct to suppress miR-24 function. In cell proliferation assays, we detected that transfection of the anti-miR-24 construct decreased cell proliferation after four days of culture (supplementary material Fig. S2E). We also performed invasion and migration assays in the MDA-MB-231 cells that expressed higher levels of miR-24 and found that expression of anti-miR-24 significantly decreased the invasive capacity (supplementary material Fig. S2F,G).

Expression of miR-24 enhanced breast cancer tumor growth, local invasion and metastasis

In order to confirm the function of miR-24, three transfected stable cell lines were injected into nude mice subcutaneously. After tumors formed, their sizes were measured regularly until the mice were sacrificed or up to 80 days. The experiments showed that tumors formed by the miR-24-cells (miR-24 tumors) grew faster than the tumors formed by the mock-transfected cells (mock tumors) or the anti-miR-24-transfected cells (anti-miR-24 tumors; Fig. 2A). During the assays, mice were sacrificed when the tumors reached the limit size set by the Animal Care Committee of Sunnybrook Research Institute. The survival curves demonstrated that miR-24 expression decreased survival rates (Fig. 2B).

The tumors were harvested, sectioned, subjected to Hematoxylin and Eosin (H&E) staining. In the mock tumors, a mixture of dead cells (showing nuclear condensation and fragmentation) and live cells were detected. Cell death was reduced in the miR-24 tumors but much higher in the Anti-miR-24 tumors than in the mock tumors (Fig. 2C). In the anti-miR-24 tumors, severe necrosis was detected in the center of the tumor. In addition, significant invasion was observed in the miR-24 tumors, showing the invasion of tumor cells into muscles. Tumor sections were also probed with anti-CD34 antibody to examine angiogenesis. We found that miR-24 expression increased tumor-associated vascularization, while anti-miR-24 expression inhibited vascularization (Fig. 2D).

We further performed tumor metastatic assays. Mock- and miR-24-transfected MT-1 cells were injected into NOD-SCID mice via tail vein, 15 in each group. Six weeks after the injection, three mice in the miR-24 group developed cachexia and four had lung metastasis in necroscopy. Typical metastatic lesions in the lungs are shown (supplementary material Fig. S2H). DNA was isolated from lung tissues and subjected to PCR to amplify the CMV promoter to indicate metastasis of the cancer cells. Expression of miR-24 promoted metastasis (Fig. 2E). Lung sections were obtained and subjected to H&E staining. Nodules were detected indicating metastasis of the tumor cells to the lungs (Fig. 2F). The miR-24-group showed multi-focal metastasis lesions in the lungs (supplementary material Fig. S2I).

miR-24 upregulated phosphorylated EGFR activities

Since activation of EGFR is tightly associated with tumor invasion and metastasis, we analyzed levels of phosphorylated EGFR (pEGFR) and EGFR in both 4T1 and MT-1 cells and observed a dramatic induction of pEGFR levels in both cell types, while the levels of EGFR were similar, suggesting activation of the existing EGFR protein (Fig. 3A; supplementary material Fig. S3A). The cell lines expressing higher levels of miR-24 produced higher levels of pEGFR (supplementary material Fig. S3B). We further analyzed pEGFR level in the tumor sections and found that the miR-24 tumors expressed higher level of pEGFR than the mock tumors (Fig. 3B). The effect of miR-24 on pEGFR expression was confirmed by western blot analysis, which showed higher levels of pEGFR in the miR-24 tumor than in the mock tumor (Fig. 3C, left). In addition, the miR-24 tumor displayed higher levels of pErk than the mock tumor (Fig. 3C, right). Lung sections prepared from mock and miR-24 mice were also analyzed for pEGFR activity. A higher level of pEGFR activity was displayed in the miR-24 lung nodules than in the mock control (Fig. 3D). On the other hand, transfection with anti-miR-24 decreased pEGFR level (supplementary material Fig. S3C).

We employed the pEGFR inhibitor AG1478 to confirm the effect of pEGFR in mediating miR-24 functions. Mock- and miR-24-transfected MT-1 cells were treated with AG1478 followed by analysis of pEGFR levels. We detected downregulation of pEGFR levels in the presence of AG1478 compared with the untreated miR-24-cells (supplementary material Fig. S3D, left).

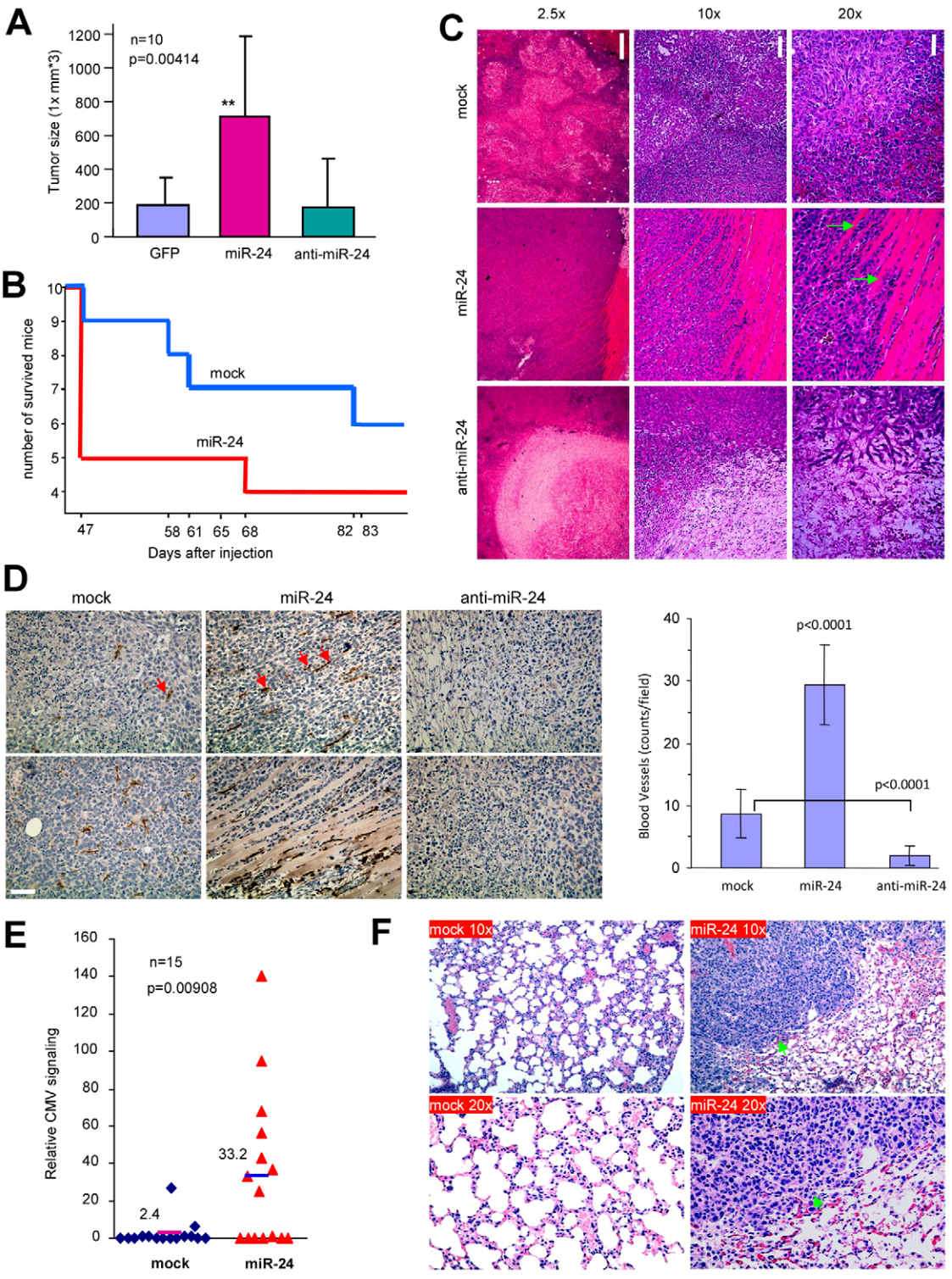

Fig. 2. Expression of miR-24 enhances breast cancer tumor growth, local invasion and metastasis. (**A**) 4T1 cells were either mock transfected, or transfected with miR-24 or anti-miR-24 and then injected subcutaneously into BALB/c mice. Expression of miR-24 enhanced tumor growth. Significant differences are indicated by asterisks. $^{**}P<0.01$. Error bars indicate the s.d. ($n=3$). (**B**) When tumors reached the maximum size allowed by Animal Care Committee, mice were sacrificed. The curve of survival indicates that miR-24 expression decreased survival rate. Since there was not much difference between the mock group and the anti-miR-24 group, only one is shown. (**C**) The tumor sections were subjected to H&E staining. In the miR-24 tumors, a mixture of tumor cells and muscles (arrows) could be seen, suggesting invasion of the tumor cells. In the anti-miR-24 tumors, extensive cell death was detected. (**D**) Left: sections of the three different tumor types were probed with anti-CD34 antibody. miR-24 expression increased tumor-associated vascularization (arrows). Scale bar: 100 µm. Right: the number of blood vessels was counted in 10 randomly selected imaging fields for statistical analysis. $n=10$. (**E**) Metastasis was estimated by isolation of DNA from lung tissues that was then subjected to PCR to amplify the CMV promoter. Expression of miR-24 promoted metastasis ($n=15$, $P=0.00908$). (**F**) H&E staining of lungs from mice injected with the mock- and miR-24-transfected cells showed metastatic lesions in the miR-24 lungs (arrows).

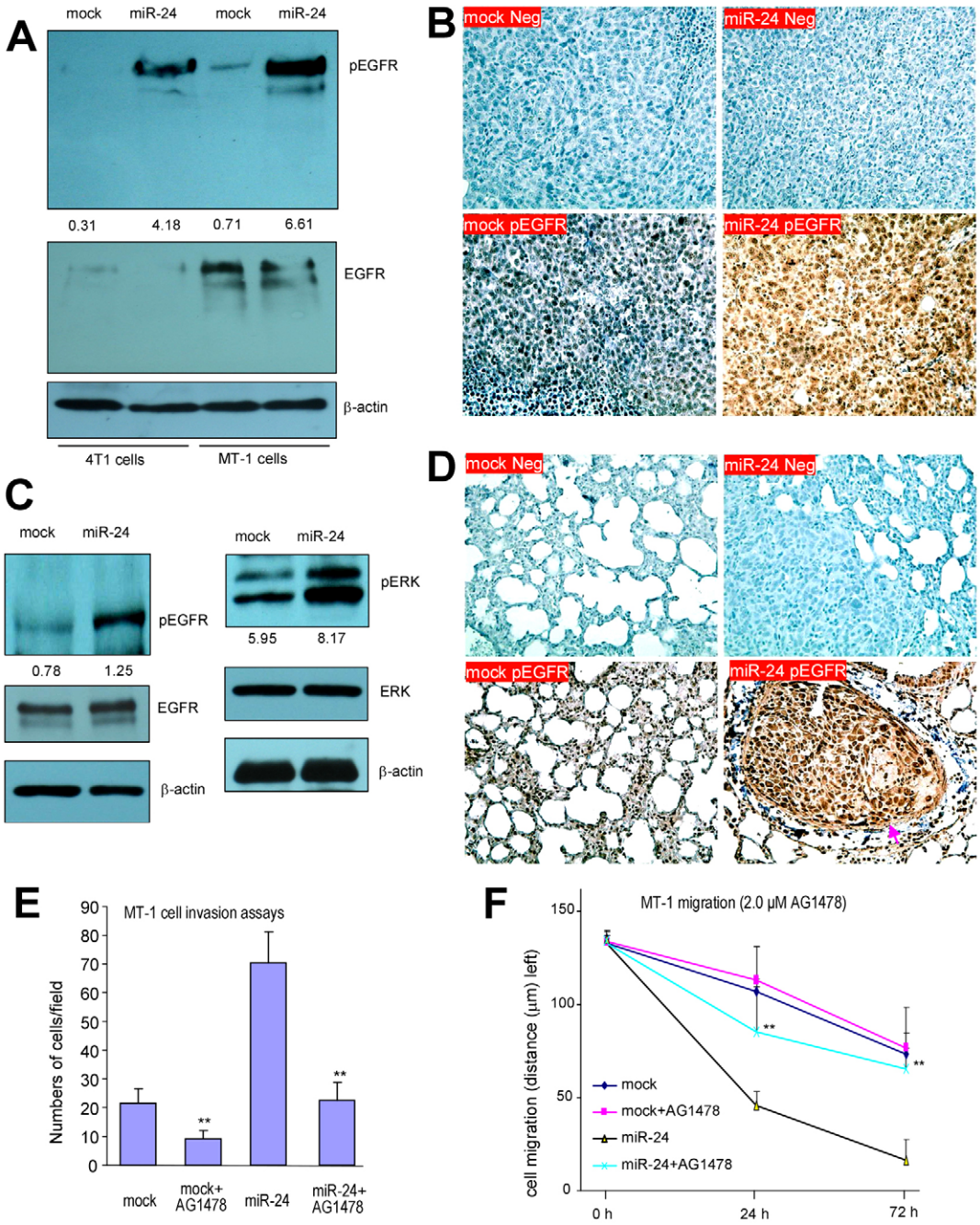

Fig. 3. miR-24 promotes pEGFR activities in breast cancer cells and tumor tissues. (**A**) Cell lysates were subjected to immunoblotting and probed with antibodies against pEGFR, EGFR and β-actin. The numbers below the gel are the relative intensities of each protein band. (**B**) Tumor sections were subjected to immunohistochemistry for pEGFR activity. Expression of miR-24 increased pEGFR levels. (**C**) Cell lysates prepared from mock and miR-24 tumors were subjected to western blot analysis and probed with antibodies against pEGFR, EGFR, pErk, Erk, and β-actin. Expression of miR-24 enhanced pEGFR and pErk activities. (**D**) Lung sections prepared from mock and miR-24 mice were subjected to immunohistochemistry for pEGFR activity. Nodules in the miR-24 lung displayed stronger pEGFR activity (arrow) than in the mock control. (**E**) Mock- and miR-24- transfected MT-1 cells (1×10^5) were incubated in medium with or without 2.0 μM AG1478 for 56 hours for cell invasion assays. Expression of miR-24 enhanced cell invasion, which was inhibited by AG1478. $^{**}P<0.01$. Error bars indicate s.d. ($n=6$). (**F**) Mock- and miR-24-transfected MT-1 cells (4×10^5) were cultured with or without 2.0 μM AG1478 for migration assays. The enhanced migration by miR-24-transfected cells was inhibited by AG1478. $^{**}P<0.01$. Error bars indicate s.d. ($n=10$).

In cell invasion assays, we found that treatment with AG1478 significantly decreased cell invasion in both the miR-24- and mock-transfected cells compared with the untreated controls (Fig. 3E; supplementary material Fig. S3E). In migration assays, we found that treatment with AG1478 significantly reduced the activities of cell migration in both the miR-24- and mock-transfected cells compared with the untreated controls (Fig. 3F; supplementary material Fig. S3F).

miR-24 targeted PTPN9 and PTPRF

To test how miR-24 exerted metastasis-promoting activities, we analyzed potential targets of miR-24 using the software miRBase (http://www.mirbase.org/cgi-bin/mirna_entry.pl?acc=MI0000080). There were a great number of candidates potentially targeted by miR-24. We focused on PTPN9 and PTPRF, two protein tyrosine phosphatases. The potential binding sites appeared at nucleotides 2333–2355 for PTPN9 and nucleotides 6111–6132 for PTPRF (Fig. 4A). We examined the levels of these proteins in 4T1 and MT-1 cells stably transfected with miR-24. In both cell lines, miR-24

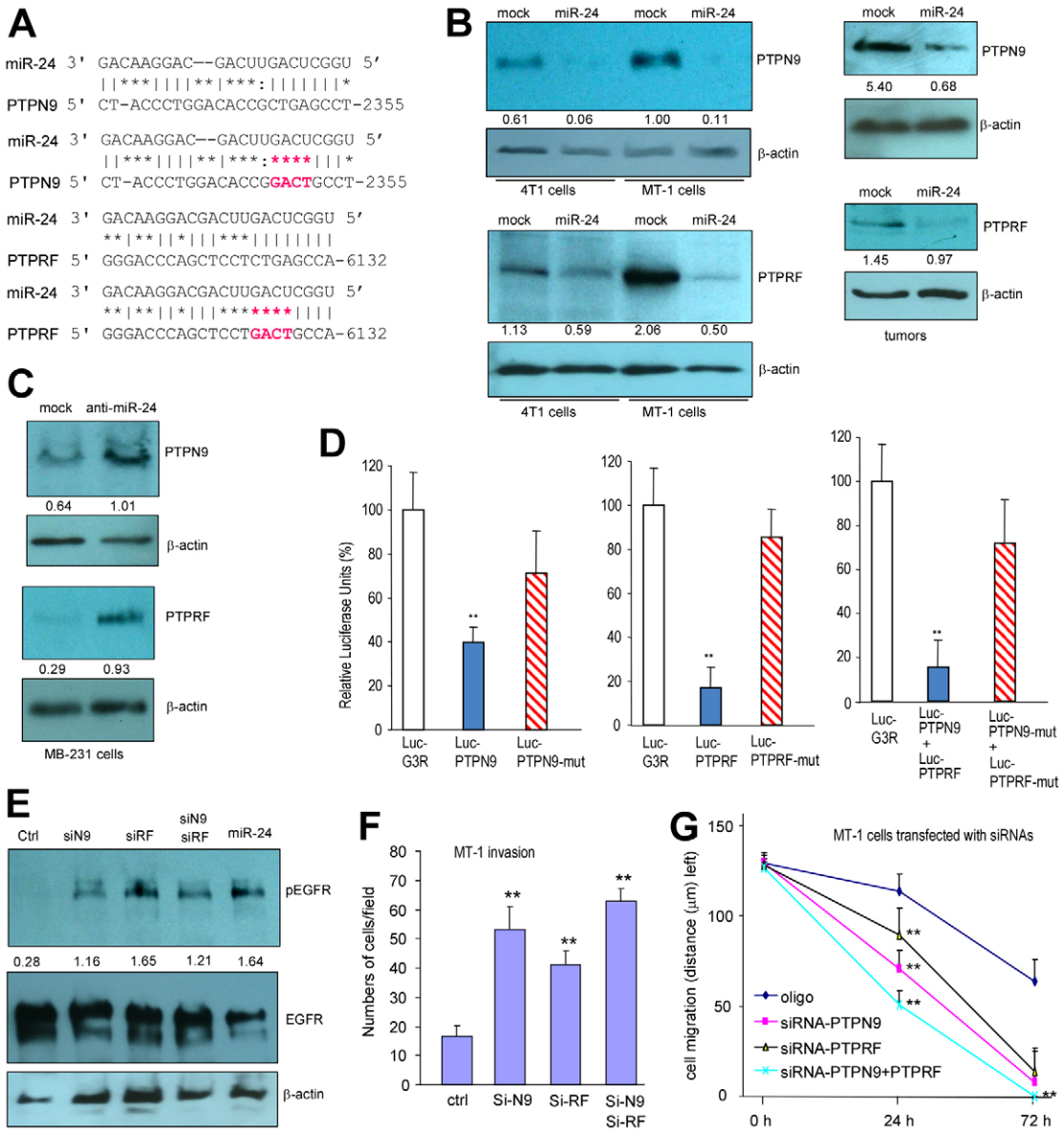

Fig. 4. miR-24 targets PTPN9 and PTPRF. (**A**) Sequences showing potential miR-24 binding sites in **PTPN9 and PTPRF**, determined by computational analysis: nucleotides 2333–2355 of PTPN9 and nucleotides 6111–6132 of PTPRF. (**B**) Cell and tumor lysates were analyzed on western blots probed with antibodies against PTPN9, PTPRF and β-actin. Repression of PTPN9 and PTPRF was detected in the cells and tumors expressing miR-24. The numbers below the gels are the relative intensities of each protein band. (**C**) Cell lysates were analyzed on western blots probed with antibodies against PTPN9, PTPRF and β-actin. Upregulation of PTPN9 and PTPRF was detected in the cells expressing the anti-miR-24 construct. (**D**) 4T1 cells were co-transfected with miR-24 and different luciferase reporter constructs. Left: the luciferase reporter construct was Luc-PTPN9 or a mutant, Luc-PTPN9-mut. The luciferase reporter vector containing a non-related sequence was used as a negative control. In the presence of PTPN9 3′UTR, the luciferase activities were inhibited, which was reversed to a significant level when the miR-24 binging site was mutated. Middle: the luciferase construct was Luc-PTPRF or a mutant Luc-PTPRF-mut. Right: The cells were co-transfected with a combination of Luc-PTPN9 and Luc-PTPRF or Luc-PTPN9-mut and Luc-PTPRF-mut. Similar results were obtained. $^{**}P<0.01$. Error bars indicate s.d. ($n=9$). (**E**) Cell lysates prepared from MT-1 cells transfected with siRNAs against PTPN9, PTPRF or a control oligo were analyzed for EGFR expression and activation. Silencing of PTPN9 or PTPRF had no effect on the expression of the other protein but enhanced EGFR phosphorylation, reaching the levels of the miR-24-transfected cells. (**F**) The cells were subject to invasion assays. Silencing PTPN9 or/and PTPRF promoted cell invasion. $^{**}P<0.01$. Error bars indicate s.d. ($n=6$). (**G**) The cells were also subjected to migration assay. Silencing PTPN9 or/and PTPRF promoted cell migration. $^{**}P<0.01$. Error bars indicate s.d. ($n=10$).

expression resulted in decreased levels of PTPN9 and PTPRF (Fig. 4B, left). Similar results were obtained in the miR-24 tumor (Fig. 4B, right). Consistent with this, transfection with anti-miR-24 increased PTPN9 and PTPFR levels (Fig. 4C). Treatment with AG1478 produced little effect on PTPN9 and PTPRF expression (supplementary material Fig. S3D, right).

To confirm the targeting of PTPN9 and PTPRF by miR-24, we performed luciferase activity assays. The luciferase reporter vector was engineered with a fragment of the 3′UTR of PTPN9 or PTPRF harboring the miR-24 target site, producing two luciferase reporter constructs Luc-PTPN9 and Luc-PTPRF (supplementary material Fig. S4A). In addition, the potential target sites were mutated as shown (Fig. 4A) producing two mutant constructs Luc-PTPN9-mut and Luc-PTPRF-mut (supplementary material Fig. S4A). Breast cancer cell line 4T1 was co-transfected with miR-24 and the luciferase reporter construct Luc-PTPN9 or Luc-PTPN9-mut. The luciferase reporter vector containing an unrelated sequence served as a negative control. The presence of the miR-24 target site reduced luciferase activities, an effect that was reduced when the target site was mutated (Fig. 4D, left). As well, co-transfection with miR-24 and Luc-PTPRF displayed significantly decreased luciferase activities compared with the control, an effect that was reversed when the target site was mutated (Fig. 4D, middle). As expected, a mixture of PTPN9 and PTPRF (50% of each) produced similar results in the luciferase activity assays (Fig. 4D, right). We also conducted the luciferase activity assays in a different cell line U343 and similar results were obtained (supplementary material Fig. S4B).

Examination of the target sequences indicated that the miR-24 target sites in the 3′UTRs of PTPN9 (supplementary material Fig. S4C) and PTPRF (supplementary material Fig. S4D) were highly conserved across different species. In all species obtained, only one nucleotide in PTPN9 and two nucleotides in PTPRF contained some deviations, while the rest were 100% homologous.

To confirm that PTPN9 and PTPRF were important in mediating the effects of miR-24 in regulating cell invasion and migration, we introduced siRNA to suppress their expression. Cell lysates prepared from MT-1 cells transfected with siRNAs against PTPN9, PTPRF or a control oligo were analyzed by western blotting to confirm appropriate RNA silencing as compared with the control (supplementary material Fig. S4E). We then analyzed EGFR expression and its activation using lysate from miR-24-transfected cells, which served as a control. Silencing of PTPN9 and PTPRF had no effect on EGFR expression but enhanced EGFR phosphorylation, reaching levels similar to those found in miR-24-transfected cells (Fig. 4E). Treatment with EGF also enhanced EGFR phosphorylation (supplementary material Fig. S4F).

MT-1 cells were treated with siRNAs against PTPN9, PTPRF, or the control oligo. The treated cells were harvested for invasion and migration assays. Silencing PTPN9 and PTPRF by treating the cells with siRNA against PTPN9 and PTPRF, respectively, promoted cell invasion (Fig. 4F; supplementary material Fig. S4G) and migration (Fig. 4G; supplementary material Fig. S4H).

Expression of pEGFR, PTPN9 and PTPRF in human breast carcinoma cell lines and patient specimens

To examine whether there was any correlation in the expression of miR-24 and its potential protein targets, we analyzed expression of pEGFR, PTPN9 and PTPRF in a number of cell lines including human breast carcinoma cells and found that expression of pEGFR was higher in the breast cancer cell lines MDA-MB468, MT-1, and MDA-MB231 than in the other cell lines tested (supplementary material Fig. S5A). Consistent with this was the lower levels of PTPN9 and PTPRF in MDA-MB468, MT-1 and MDA-MB231. Interestingly, the levels of miR-24 were also higher in these cell lines than the other cell lines (supplementary material Fig. S5B), suggesting a potential role of miR-24 in repressing PTPN9 and PTPRF expression in these cells, resulting in promotion of EGFR activity.

We then examined expression of pEGFR, PTPN9 and PTPRF in human breast carcinoma specimens. We found that expression of pEGFR was much higher in human breast carcinoma specimens than in the normal breast tissues (Fig. 5; supplementary material Fig. S5C). On the other hand, expression of PTPN9 and PTPRF was much weaker in the tumor tissues than in the normal tissue (Fig. 5A; supplementary material Fig. S5D,E). Double staining confirmed that expression of pEGFR was stronger than expression of PTPN9 and PTPRF in the tumor tissues, which was opposite to what was found in the normal tissues (supplementary material Fig. S6). The sections were probed for miR-24 expression using the miRCury LNA microRNA ISH Optimization Kit from Exiqon. We detected high levels of miR-24 expression in the cancer cells but not in the normal ductal structure of the breast (Fig. 5B).

PTPN9 and PTPRF rescued the effects of miR-24

To further confirm that PTPN9 and PTPRF played essential roles in mediating miR-24 effect, we conducted rescue experiments. The retroviral vector pBABE was engineered with the coding sequences of either PTPN9 or PTPRF (supplementary material Fig. S7A). MT-1 cells were transfected with PTPN9 combined with miR-24, PTPRF combined with miR-24, miR-24 alone or were mock transfected and then analyzed by western blotting. As expected, transfection with PTPN9 and PTPRF increased their expression respectively, which resulted in decreased pEGFR levels (Fig. 6A).

Invasion assays were performed on MT-1 cells transfected with PTPN9 combined with miR-24, PTPRF combined with miR-24, miR-24 alone or the mock construct. Enhanced cell invasion induced by miR-24 expression was abolished by transfection with PTPN9 and PTPRF (Fig. 6B; supplementary material Fig. S7B). The cells were also cultured to sub-confluence before being utilized in wound healing and migration assays. Enhanced cell migration by miR-24 expression was abolished by transfection with PTPN9 and PTPRF (Fig. 6C; supplementary material Fig. S7C). Ectopic expression of PTPN9 and PTPRF also abolished the effects of miR-24 on cell proliferation (supplementary material Fig. S7D) and colony formation (supplementary material Fig. S7E). The rescue effects of PTPN9 and PTPRF were also confirmed in another breast cancer cell line 4T1. Ectopic expression of PTPN9 and PTPRF reduced activation of pEGFR (supplementary material Fig. S7F), resulting in decreased cell invasion (supplementary material Fig. S7G), cell proliferation (supplementary material Fig. S8A), migration (supplementary material Fig. S8B) and colony formation (supplementary material Fig. S8C).

The MT-1 cells stably infected with pBABE-PTPN9 and pBABE-PTPRF were subjected to metastasis assays. After being sacrificed, the mice were examined for nodules in the lung. Lung tissues were harvested for DNA isolation followed by real-time PCR analysis to quantify ectopic DNA in the lung, which is a

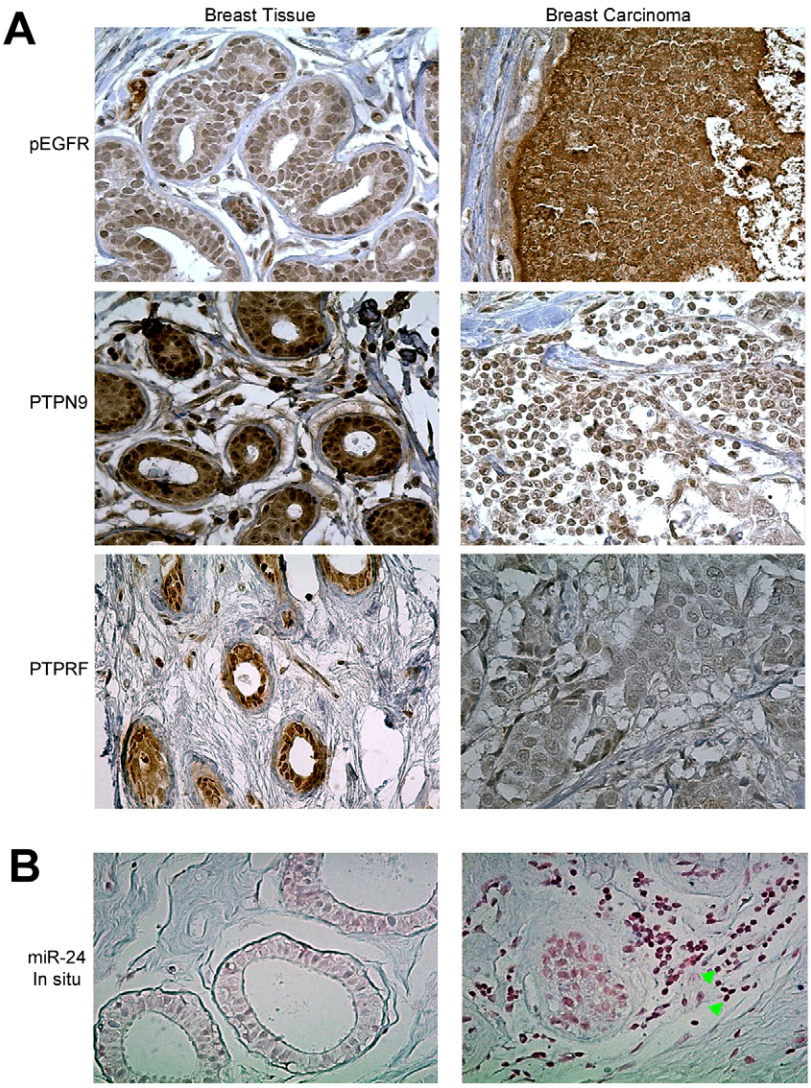

Fig. 5. Expression of pEGFR, PTPN9, PTPRF and miR-24 in human breast carcinoma. (**A**) Sections from human breast carcinoma and normal tissues were subjected to immunohistochemistry for activities of pEGFR, PTPN9 and PTPRF. The levels of pEGFR were higher whereas those of PTPN9 and PTPRF were lower in the tumor tissue than in the normal duct tissues. (**B**) The sections were also probed for miR-24 expression. High levels of miR-24 were detected in the cancer cells (green arrows) but not in the normal ductal structure of the breast.

sign of metastasis. The experiments indicated that there were significantly higher levels of metastasis in the miR-24-treated mice than that in the mock-treated mice (Fig. 6D). Ectopic expression of PTPN9 or PTPRF decreased metastasis significantly. The tissues were also subjected to sectioning and H&E staining. We found nodules in the miR-24-treated mice but not in the mock-treated or in the PTPN9- and PTPRF-treated mice (Fig. 6E). The lung sections were immunostained for expression of PTPN9 and PTPRF to confirm metastasis of tumor cells (supplementary material Fig. S8D) and activation of pEGFR. We found that ectopic expression of PTPN9 and PTPRF abolished the increased expression of pEGFR by miR-24 (Fig. 6F).

Overexpression of miR-24 enhanced EGFR signaling and its down-stream pathways

We finally investigated the signaling pathway mediating the effects of miR-24. Cell lysates from miR-24- or mock-transfected MT-1 cell were analyzed by western blotting and probed for expression of MMP2, MMP11, ADAM15, TIMP2 and TIMP3. We detected upregulation of MMP2, MMP11 and ADAM15, but downregulation of TIMP2 in the cells (Fig. 7A). Expression of TIMP3 was not affected. To corroborate these results, we transfected MDA-MB-231 cells with anti-miR-24 and mock constructs, followed by western blot analysis of the expression of MMP2, MMP11, ADAM15, TIMP2 and TIMP3. Opposite to the above results, we detected downregulation of MMP2, MMP11 and ADAM15 but upregulation of TIMP2 in the cells (Fig. 7B).

To confirm that the up- and downregulation of these proteins was the consequence of miR-24 targeting PTPN9 and PTPRF and activation of pEGFR, we treated the mock- and miR-24-transfected MT-1 cells with 2.0 μM AG1478. Expression of the above proteins was analyzed by western blot analysis. We detected downregulation of MMP2, MMP11 and ADAM15 but upregulation of TIMP2 in the miR-24-transfected cells (supplementary material Fig. S9A). We confirmed that expression of pEGFR, MMP2, MMP11 and ADAM15 was upregulated while expression of PTPN9, PTPRF and TIMP2 was downregulated in the miR-24 tumors as compared with the mock tumors (supplementary material Fig. S9B). Upregulation of MMP2, MMP11, AMAD15 and pErk, while downregulation of TIMP2 was also detected in human breast carcinoma tissues compared with the normal duct structures in the breast (supplementary material Fig. S9C).

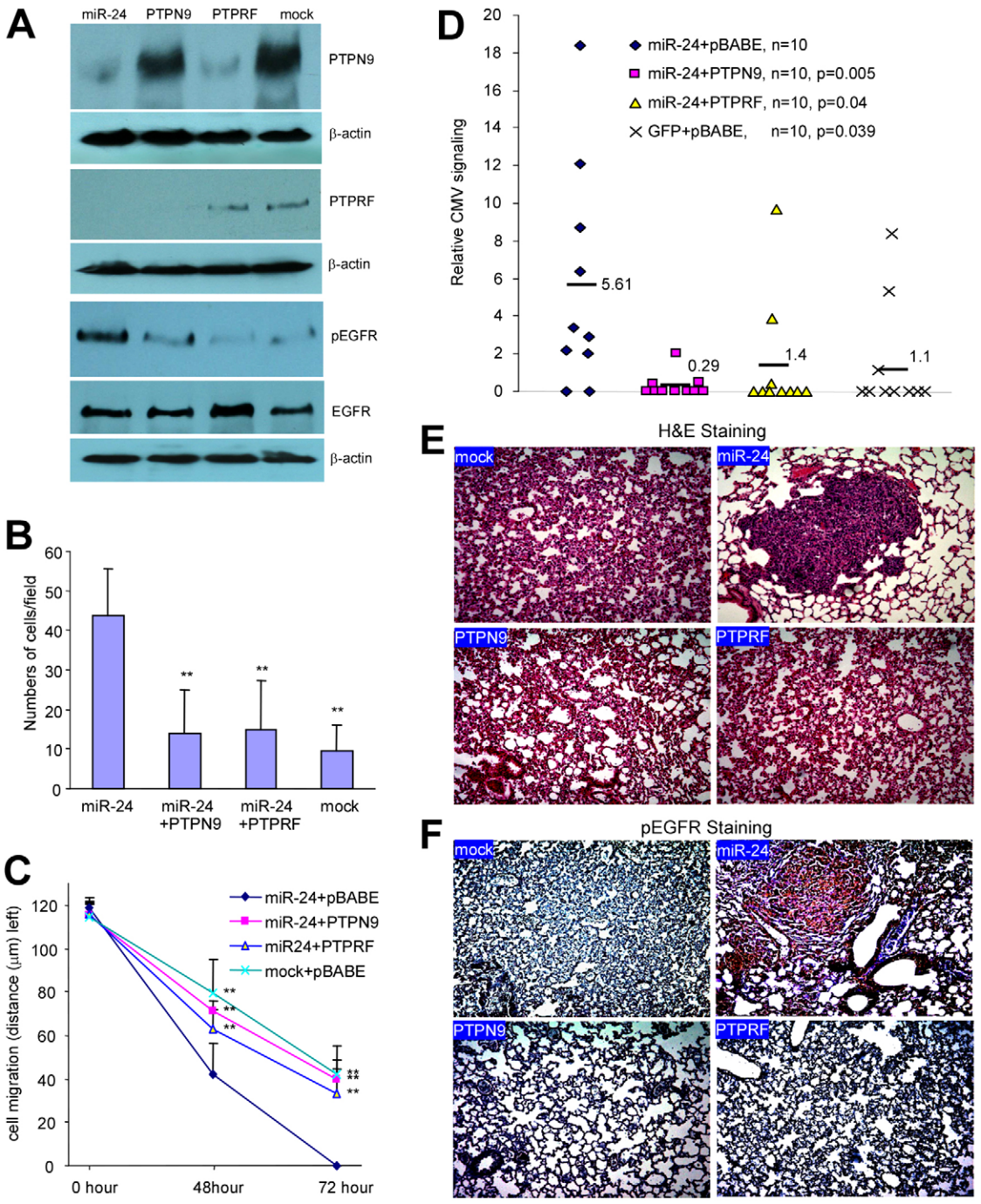

Fig. 6. Rescue miR-24 effects. (**A**) Cell lysates prepared from MT-1 cells that were mock transfected or transfected with miR-24, miR-24 and PTPN9, or miR-24 and PTPRF were analyzed for expression and activation of PTPN9, PTPRF and EGFR. Transfection with PTPN9 and PTPRF increased their expression, respectively, which resulted in a decrease in pEGFR levels. (**B**) Cell invasion assays were performed with cells treated as in A (1×10^5). Enhanced cell invasion by miR-24 expression was abolished by transfection with PTPN9 and PTPRF. $^{**}P<0.01$. Error bars indicate s.d. ($n=8$). (**C**) Migration assays showed that enhanced cell migration by miR-24 expression was abolished by transfection with PTPN9 and PTPRF. $^{**}P<0.01$. Error bars indicate s.d. ($n=10$). (**D**) DNA was isolated from lung tissues and subjected to PCR to amplify the CMV promoter as an indicator of metastasis. The enhanced metastasis by miR-24 was inhibited by ectopic expression of PTPN9 and PTPRF. ($n=10$). (**E**) H&E-stained sections showing that ectopic expression of PTPN9 and PTPRF inhibits metastasis in the lung. (**F**) Lung tissues were subjected to immuno-staining with pEGFR antibody. The increased pEGFR level resulting from miR-24 expression was inhibited by PTPN9 and PTPRF.

To understand the signaling pathway by which miR-24 functioned, we produced a figure to show how miR-24 possibly acts in breast cancer invasion and metastasis (Fig. 7C). In brief, miR-24 targeted PTPN9 and PTPRF, and downregulated expression of PTPN9 and PTPRF, which in turn activated EGFR (pEGFR). Increased pEGFR activity promoted expression of MMP2 and MMP11, which partly

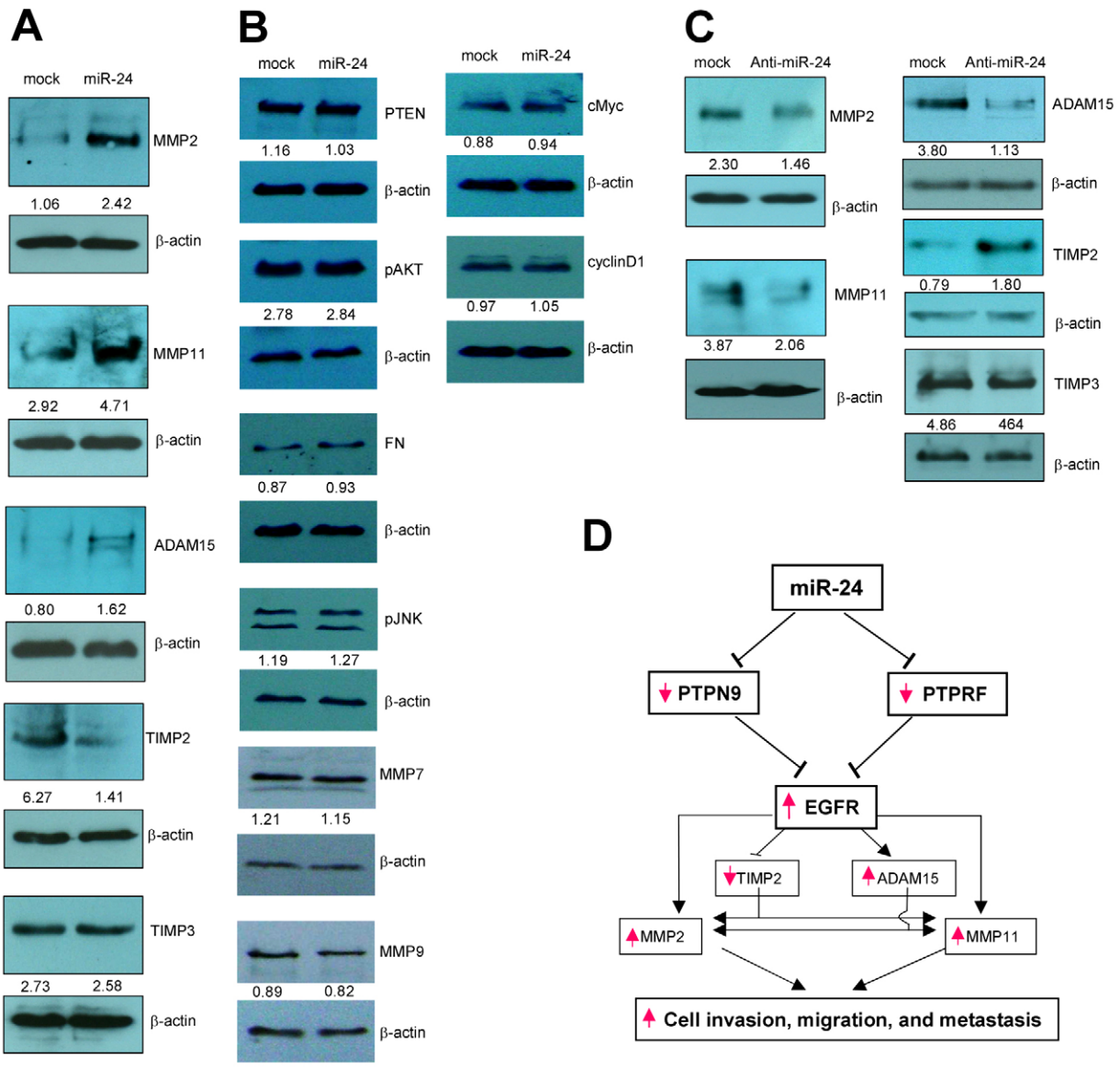

Fig. 7. Overexpression of miR-24 enhances EGFR signaling and its downstream pathways. (**A**) Cell lysates from mock- or miR-24-transfected MT-1 cells were analyzed on western blots probed for expression of MMP2, MMP11, ADAM15, TIMP2, TIMP3 and β-actin. Upregulation of MMP2, MMP11 and ADAM15 and downregulation of TIMP2 was detected. (**B**) Expression of some unrelated proteins was also analyzed. (**C**) Cell lysates from mock- or miR-24-transfected MDA-MB-231 cells were analyzed by western blotting for expression of MMP2, MMP11, ADAM15, TIMP2 and TIMP3. Downregulation of MMP2, MMP11, and ADAM15 and upregulation of TIMP2 was detected. (**D**) The potential function of miR-24 in breast cancer invasion and metastasis is shown in the diagram. miR-24 targets PTPN9 and PTPRF and downregulates their expression, which in turn activates EGFR (pEGFR). The increased pEGFR activity promotes expression of MMP2 and MMP11, which partially downregulates expression of TIMP2 and upregulates expression of ADAM15. As a consequence, increased expression of MMP2 and MMP11 enhances breast cancer cell migration, invasion and metastasis.

downregulated the expression of TIMP2 and upregulated the expression of ADAM15. As a consequence, increased expression of MMP2 and MMP11 enhanced breast cancer cell migration, invasion and metastasis. Thus, miR-24 represses PTPN9 and PTPRF, which coordinately regulate EGFR to mediate miR-24 functions. In an accompanying paper, we demonstrate that miR-17, producing miR-17-5p and miR-17-3p, represses PTEN, GalNT7 and vimentin. These targets, although functioning in different signal pathways, can mediate miR-17 functions coordinately, leading to the development of hepatocellular carcinoma (see Shan et al., 2013 in this issue of *Journal of Cell Science*).

Discussion

Our study demonstrated that miR-24 was highly expressed in human breast carcinoma. This suggested a role of miR-24 in cancer development/progression, which was consistent with previous studies showing that miR-24 was highly expressed in patients with gastric cancer and lung cancer (Xie et al., 2011), cervical cancer (Wang et al., 2008b) and oral carcinoma (Lin et al., 2010). MiR-24 has also been reported to target p16, a tumor suppressor (Lal et al., 2008). We found that expression of miR-24 promoted tumor growth, invasion and metastasis by upregulating EGFR activity due to its suppressive effect on

PTPN9 and PTPRF, two phosphatases of EGFR. Rescue experiments expressing these phosphatases reversed the effects of miR-24 on tumor cell invasion and metastasis. Currently reported miR-24 functions include promotion of cell proliferation (Zaidi et al., 2009) and inhibition of apoptosis in cancer cells (Qin et al., 2010) and cardiomyocytes (Qian et al., 2011). This may be due to its capacity in repressing a great number of potential genes (368 candidate targets being predicted at http://pictar.mdc-berlin.de/cgi-bin/PicTar_vertebrate.cgi?action=Search%20for%20targets%20of%20a%20miRNA&name2=hsa-miR-24). In addition, miR-24 has been reported to target some 'seedless' 3′UTRs (Lal et al., 2009). Initially reported ten years ago (Lagos-Quintana et al., 2001), the roles of miR-24 are only starting to be recognized in a variety of cells and tissues.

To dissect the signaling pathway associated with miR-24 promotion of tumor growth, invasion and metastasis, we examined expression of a number of oncogenes and tumor suppressors and found that EGFR was strongly activated in the miR-24 expressing cells and tumors. As a cell surface receptor, EGFR transitions from an inactive state to an active state by autophosphorylation of its tyrosine residues (Swanton et al., 2008). Phosphorylation of EGFR results in activation of downstream MARK, ERK, Akt and JNK signaling pathways leading to DNA synthesis, cell proliferation and cell migration (Schmidt-Ullrich et al., 1997; Sørensen et al., 2006). Thus, phosphorylated EGFR plays important roles in tumor invasion and metastasis (Arora and Simpson, 2008; Gong et al., 2008). Over-activation of EGFR including constant activation and mutations is often associated with cancer development and progression (Lynch et al., 2004; Walker et al., 2009). Our results showing that EGFR was strongly activated upon miR-24 overexpression appeared to be a consequence of miR-24 repressing PTPN9 and PTPRF expression. Consistent with these results were the activation of Erk, ADAM15, MMP2 and MMP11 and downregulation of TIMP2 levels, which supported a role of EGFR in mediating miR-24 activities.

Since EGFR was not a target of miR-24, we reasoned that miR-24 may have targeted the endogenous inhibitors for EGFR phosphorylation such as the protein tyrosine phosphatases (PTPs). Due to their critical roles in physiology and tissue development, a great number of PTPs were expressed in various cell types, and the activity of each PTP was tightly controlled. PTPN9 is a non-receptor type 9 phosphatase in the cytoplasm, playing a role in intracellular secretory vesicle fusion (Huynh et al., 2004). PTPN9 has been reported to inhibit EGFR signaling by dephosphorylating EGFR leading to impaired growth and invasion of breast cancer cells (Yuan et al., 2010). We showed in this study that miR-24 could promote EGFR functions by repressing PTPN9 expression. Our results confirmed the function of PTPN9 in dephosphorylating EGFR as reported (Yuan et al., 2010) and added an additional layer to the regulation of PTPN9 expression, namely the regulation of PTPN9 by miR-24. This regulation appears to be significant in breast carcinoma patients who express high levels of EGFR. We found that approximately two-thirds of breast cancer patients express high levels of miR-24 and that most of the breast carcinoma specimens displayed high levels of pEGFR. Whether or not these patients expressed high levels of activated EGFR awaits further investigation. In addition, our results demonstrated that in human breast cancer cell lines, both EGFR and miR-24 were highly expressed while PTPN9 was downregulated, suggesting a possible inhibitory role of miR-24 in PTPN9 expression while promoting EGFR activity (e.g. enhanced EGFR phosphorylation).

Furthermore, we demonstrated that PTPRF was another target of miR-24. PTPRF is a receptor-type F protein tyrosine phosphatase. Although the function of PTPRF is not clear, it has been reported that PTPRF plays a role in mesenchymal stem cell self-renewal (Song and Tuan, 2006). There have been no reports on the role of PTPRF in dephosphorylating EGFR. In this study, we showed a reverse correlation between pEGFR and PTPRF levels. These results suggested that PTPRF may dephosphorylate EGFR in these cells. In clinical specimens, we also detected an inverted relationship between PTPRF and pEGFR levels, supporting a role of PTPRF in EGFR dephosphorylation. Knockdown of PTPRF increased pEGFR levels leading to enhanced cell invasion and migration. Ectopic expression of PTPRF decreased pEGFR levels, cell invasion, migration and tumor metastasis to the lung. These results directly supported the role of PTPRF in the inhibition of EGFR activities. The precise manner by which PTPRF dephospohrylates EGFR, awaits further investigation.

Materials and Methods

Materials

The monoclonal antibodies against ERK2, pERK, and the polyclonal antibodies against EGFR, pEGFR, PTPN9, PTPRF, MMP2, MMP11 and ADAM15 were obtained from Santa Cruz Biotechnology. EGF, selective EGFR inhibitor AG1478, mytomycin, and the monoclonal antibody against β-actin used were obtained from Sigma. The polyclonal antibodies against TIMP2 and TIMP3 were obtained from Abcam. Horseradish peroxidase-conjugated goat anti-mouse IgG and horseradish peroxidase-conjugated goat anti-rabbit IgG were obtained from Bio-Rad. Immunoblotting was performed using the ECL Western Blot detection kit. Cell Proliferation Reagent WST-1 and High Pure PCR Template Preparation kits were obtained from Roche Applied Science. The MT-1 cells used in this study was originally described by Naundorf and co-workers (Naundorf et al., 1992), while 4T1 cells were described by Aslakson and Miller (Aslakson and Miller, 1992).

Construct generation

Plasmid miR-24 and control plasmid were generated which have GFP and selected antibiotics marker respectively. Both plasmids contain a Bluescript backbone, a CMV promoter driving green fluorescent protein (GFP) expression and a human H1 promoter driving pre-miR-24 or a non-related sequence serving as a control. The control plasmid was the same as the miR-24 construct except the pre-miR-24 sequence was replaced with a non-related sequence (5′-atacagtactgtgataactgaagtttttggaaaagctttagttattaa-3′), serving as a mock control. In order to analyze the function of miR-24, the two constructs were transfected into 4T1 cells. After cell sorting through monitoring GFP signal by FACS (fluorescence activated cell sorter), transfected stable cells were obtained and used in this study.

A luciferase reporter vector (pMir-Report; Ambion) was used to generate the luciferase constructs. A fragment of the 3′-untranslated region (3′UTR) of human PTPN9 or PTPRF was cloned by RT-PCR. Two primers, huPTPN9-SacI (5′-cccgagctcctctcctacgaacctcctacc-3′) and huPTPN9-MluI (5′-cccacgcgtggcaaatgctcatcaaacctcccc-3′), were synthesized to clone the 3′UTR fragment of PTPN9, while the 3′UTR fragment of PTPRF was cloned with the primers huPTPRF-SacI (5′-cccgagctcctaccgctcccctctcctccgccac-3′) and huPTPRF-MluI (5′-cccacgcgtggattcgcgaaaggaaaaatcagag-3′). The PCR products were digested with *Sac*I and *Mlu*I and the fragments were inserted into a *Sac*I- and *Mlu*I-opened pMir-Report Luciferase vector to obtain the luciferase constructs, Luc-PTPN9 and Luc-PTPRF, respectively. Mutations of the miR-24 binding sites were also created, which was derived by PCR approach, using two primers huPTPN9-SacI-mut (5′cccgagctcctctcctacgaacctcctacctgttggccagccttccttaaactaccctggacaccggactgcct-3′) and huPTPN9-MluI to generate a mutant construct Luc-PTPN9-mut, and two primers huPTPRF-SacI-mut (5′-cccgagctc ctaccgctcccctctcctccgccacccccgccgtggggctccggaggggaccca-gctcctgactgcca-3′) and huPTPRF-MluI to generate Luc-PTPRF-mut. To serve as a negative control, a non-related sequence was amplified from the coding sequence of the chicken versican G3 domain using two primers, chver10051SpeI and chver10350SacI (Shan et al., 2009). We do not expect any endogenous miRNA to bind to this fragment as it is in a coding region.

To generate PTPN9 expression construct, we amplified the PTPN9 coding sequence (access number NM_002833.2, 1782 base pairs) by PCR with pfu polymerase and two primers (Ptpn9-For, 5′-ccccgaattcgagcccgcgaccgcgccc-3′ and Ptpn9-Rev, 5′-ccccgtcgacttactgactctccacggc-3′). The PCR fragment was cloned at *Eco*RI and *Xho*I sites in a Myc-tagged pCDNA3.1 expression vector. After confirmation of the correct sequence, the 1782-bp *Hin*dIII and *Xba*I fragment was released from this plasmid and treated with Klenow enzyme to produce blunt end and sub-cloned at *Sna*BI of pBabe-puro retroviral vector.

To generate PTPRF expression construct, we performed the amplification with two primers (Ptprf-For, 5′-ccccggtaccatggcccctgagccagcc-3′ and Ptprf-Rev, 5′-ccccgcggccgcccgttgcatagtggtcaaa-3′). This 5694-bp fragment was cloned at *Bam*HI and *Sac*II sites in pBS SK vector. After confirmation of the correct sequence, the fragment was obtained with the restriction enzymes *Kpn*I and *Sac*II from pBS vector and sub-cloned at *Kpn*I and *Sac*II sites in pCDNA4/myc-HisB. An *Eco*RV and *Age*I fragment from the PTPRF-pCDNA4/myc-HisB plasmid was released and treated with Klenow enzyme to produce blunt end and sub-cloned at the *SnaB*I of pBabe-puro retroviral vector.

Production of stable cell lines

The plasmids pBabe-PTPN9 and pBabe-PTPRF were transfected into Hek293T cells to produce retrovirus. Harvested retroviruses in the cultural media were mixed with 6 μg/ml of polybrene (Sigma) and added into culture dishes to infect cells. 24 hours after infection, cells were trypsinized and diluted into 96-well plates and selected with 2 μg/ml of Puromycin (Invitrogen). Individual clones were screened by western blotting with anti-Myc antibody (Sigma).

Cell proliferation assay

The method was as described previously (Deng et al., 2013).

Cell survival assay

The method was as described previously (Yang et al., 2012).

Mammosphere formation

Harvested mock- and miR-24-transfected cells were mechanically and enzymatically dissociated in 0.05% Trypsin-EDTA at 37℃ for 10 minutes, followed by resuspension in serum-free DMEM/F12 medium containing 10 ng/ml bFGF, 20 ng/ml EGF, L-glutamine (1:400) and B27 supplement (1:50). Single cell suspensions were plated in 60-mm Petri dishes at 1000 cells/well. After culturing for additional 3 days, sphere cells were collected by gentle centrifugation, dissociated to single cells in 0.05% trypsin-EDTA and then cultured to generate mammospheres of the next generation.

Cell migration assays

We performed two different cell migration assays. In the wound-healing experiment, the method was performed as described (Rutnam and Yang, 2012b). The other migration assay was performed with the modified chemotactic Boyden chamber motility assays, which was performed using 24-well cell culture plates and a 3 μm cell culture insert. The lower chamber of the Transwell was filled with 600 μl of 10% fetal bovine serum (FBS)/DMEM and incubated at 37℃ for 2 hours. Mock- and miR-24-transfected cells (1×10^5) in 100 μl serum-free DMEM were gently injected onto each filter insert (upper chamber) and then incubated at 37℃ for 4 hours. The filter inserts were removed from the chambers, fixed with methanol for 5 minutes and stained with Harris' Hemotoxylin for 20 minutes. Samples were subsequently washed, dried and mounted onto slides for analysis using a light microscope. Migrating cells were stained blue and were counted in six fields of views/membrane.

Cell invasion assay

Cell invasion assay was performed with the modified chemotactic Boyden chamber invasion assays using 24-well cell culture plates and an 8 μm cell culture insert as described previously (Rutnam and Yang, 2012b).

Colony formation in soft agarose gel

The method was described previously (Deng et al., 2013).

Western blot analysis

Western blotting was performed as described previously (LaPierre et al., 2007).

Cell cycle analysis

Mock- and miR-24-transfected cells were washed and resuspended in cold PBS and incubated in ice-cold 70% ethanol for 3 hours. The cells were then centrifuged at 1500 rpm for 10 minutes and resuspended in propidium iodide (PI) master mix (40 mg/ml PI and 100 mg/ml RNase in PBS) at a density of 5×10^5 cells/ml and incubated at 37℃ for 30 minutes before analysis with flow cytometry.

Luciferase activity assay

Luciferase activity assay was performed using a dual-luciferase reporter system developed by Promega (E1960). This method was performed as described previously (Jeyapalan et al., 2011).

Real-time PCR

This was performed as previously described (Lee et al., 2009). The primers used as real-time PCR controls were human-U6RNAf and human-U6RNAr.

In vivo tumorigenicity in BALB/c mice, local tumor growth and invasion

The method was described recently except that each group contained 10 mice (Fang et al., 2012b). At necroscopy, primary tumors, stromal tissues, lungs, liver, spine were dissected. Half of the organs were fixed in 10% formalin and the other half were frozen in liquid nitrogen for subsequent analysis. The animal experiments were performed according to the guideline approved by the Animal Care Committee at Sunnybrook Research Institute.

In vivo tumorigenicity in nude mice, lung metastasis

The mock- and miR-24-tansfected MT-1 cells were cultured in 10% FBS/RPMI 1640 media at 37℃ with 5% CO_2. At 70% to 80% subconfluency, the cells were given fresh 10% FBS/RPMI 1640 media 24 hours before being introduced into the mice. Cell viability was determined and cells were suspended with greater than 95% viability without cell clumping. Four-week-old nude mice were injected in the tail vein with the above transfected cells (2×10^5 cells in 150 μl 10% FBS/RPMI 1640 medium). Each group had 15 randomly selected mice. All mice were sacrificed 6 weeks after injection. At necroscopy, lungs, liver, spines were dissected. Half the organs were fixed in 10% formalin and the other half were frozen in liquid nitrogen for subsequent analysis.

Mouse lung tissues were homogenized and the genomic DNAs were isolated with High Pure PCR Template Preparation kit according to the manufacturer's instructions. In order to estimate tumor burden, we extracted three samples from the above organs of each animal. Tumor burden for each individual tissue was measured using real-time PCR. Primers used were as follows: CMV forward (5′-gtcatcgctattaccatggtgatgcgg-3′) and CMV reverse (5′-agctctgcttatatagacctcccaccg-3′) for genotyping; β-actin forward (5′-ccggcatgtgcaaagccggcttcg-3′) and β–actin reverse (5′-ctcattgtagaaggtgtggtgcc-3′) for loading control.

Tissue H&E staining, immunohistochemistry

Primary tumors or lungs were freshly excised and fixed in 10% formalin overnight, immersed in 70% ethanol, embedded in paraffin, and sectioned. The sections were subjected to Hematoxylin and Eosin (H&E) staining and immunohistochemistry and were de-paraffinized with xylene and ethanol and then boiled in a pressure cooker. After washing with Tris-buffered saline (TBS) containing 0.025% Triton X-100, the sections were blocked with 10% goat serum and incubated with primary antibody in TBS containing 10% goat serum albumin overnight. The sections were washed and labeled with biotinylated secondary antibody, followed by avidin-conjugated horseradish peroxidase provided by the Vectastain ABC kit (Vector, PK-4000). The slides were subsequently stained with DAB followed by Mayer's Hematoxylin for counter staining and slide mounting.

For multiple antigen staining, an avidin/biotin blocking kit (SP-2001) was used to prevent the interaction of the second set of labeling reagents with the first set of labeling reagents. Briefly, the sections were incubated with Avidin solution for 15 minutes and then incubated in Biotin Solution for 15 minutes. After washing with Tris-buffered saline (TBS) containing 0.025% Triton X-100, the sections were blocked with 10% goat serum and incubated with primary antibody to second antigen and followed by each step as the first staining.

Clinical specimens

Breast specimens were collected at the time of mastectomy from previously untreated patients, fixed in 10% formalin overnight, immersed in 70% ethanol, embedded in paraffin and sectioned. Corresponding normal tissue was obtained from the same mastectomy specimen as the tumor, from a different quadrant of the breast. The tissue blocks were confirmed with examination under light microscopy by a pathologist and confirmed to be benign or malignant based on histology of the corresponding H&E stained slide. Sections were subjected to immuno-histochemistry probed with antibodies against EGFR, pEGFR, PTPN9 and PTPRF. The work was conducted following a protocol approved by the Institutional Review Board at the University of Iowa Carver College of Medicine and a protocol approved by the Affiliated People's Hospital of Jiangsu University.

Experiments using freshly frozen clinical specimens were also conducted independently in the Affiliated People's Hospital of Jiangsu University according to a protocol approved by the Clinical Research Ethics Committee at the Hospital. In brief, small RNAs were isolated from formalin-fixed, paraffin-embedded tissue blocks, using the Total Nucleic Acid Isolation Kit (Ambion) or from freshly frozen tissues. Quantification of miRNAs was performed with real-time PCR.

Statistical analysis

The results (means values ± s.d.) of all the experiments were subjected to statistical analysis using Student's *t*-tests. The level of significance was set at $P<0.01$.

Author contributions

W.W.D. performed most of the cell biology experiments, western blot analyses and luciferase assays, and was involved in tumor

formation assays, data analysis and paper writing. L.F. was involved in animal dissecting analysis, directed pathological analysis and some immunostaining. M.L. helped W.W.D. to initiate the project and was involved in some tumor formation assays. X.Y. performed some immunostaining. Y.L. generated PTPN9 and PTPRF expression constructs, and cell lines. C.P. supervised Y.L.′s work. W.Q., Y.Q.O., R.W.A., S.L.S., J.Q., J.L., provided patient specimens. Z.J., A.J.Y. and M.S. were aware of the experiments and involved in discussion. Z.D. performed real-time PCR. S.W.S. was involved in generating luciferase constructs. C.-H.W. was involved in generating miR-24 expression construct. B.B.Y. designed and supervised the project, analyzed the results, and wrote the paper.

Funding

This work was supported by the Canadian Institutes of Health Research [grant numbers MOP-102635 and MOP-111171 to B.B.Y. and MOP-89931 to CP], and a Career Investigator Award from the Heart and Stroke Foundation of Ontario [grant number CI 7418 to B.B.Y.].

Supplementary material available online at
http://jcs.biologists.org/lookup/suppl/doi:10.1242/jcs.118299/-/DC1

References

Arora, A. and Simpson, D. A. (2008). Individual mRNA expression profiles reveal the effects of specific microRNAs. *Genome Biol.* **9**, R82.

Aslakson, C. J. and Miller, F. R. (1992). Selective events in the metastatic process defined by analysis of the sequential dissemination of subpopulations of a mouse mammary tumor. *Cancer Res.* **52**, 1399-1405.

Deng, M., Tang, H., Zhou, Y., Zhou, M., Xiong, W., Zheng, Y., Ye, Q., Zeng, X., Liao, Q., Guo, X. et al. (2011). miR-216b suppresses tumor growth and invasion by targeting KRAS in nasopharyngeal carcinoma. *J. Cell Sci.* **124**, 2997-3005.

Deng, Z., Du, W. W., Fang, L., Shan, S. W., Qian, J., Lin, J., Qian, W., Ma, J., Rutnam, Z. J. and Yang, B. B. (2013). The intermediate filament vimentin mediates microRNA miR-378 function in cellular self-renewal by regulating the expression of the Sox2 transcription factor. *J. Biol. Chem.* **288**, 319-331

Fang, L., Deng, Z., Shatseva, T., Yang, J., Peng, C., Du, W. W., Yee, A. J., Ang, L. C., He, C., Shan, S. W. et al. (2011). MicroRNA miR-93 promotes tumor growth and angiogenesis by targeting integrin-β8. *Oncogene* **30**, 806-821.

Fang, L., Du, W. W., Yang, W., Rutnam, Z. J., Peng, C., Li, H., O'Malley, Y. Q., Askeland, R. W., Sugg, S., Liu, M. et al. (2012a). MiR-93 enhances angiogenesis and metastasis by targeting LATS2. *Cell Cycle* **11**, 4352-4365.

Fang, L., Du, W. W., Yang, X., Chen, K., Ghanekar, A., Levy, G., Yang, W., Yee, A. J., Lu, W. Y., Xuan, J. W. et al. (2012b). Versican 3′-untranslated region (3′-UTR) functions as a ceRNA in inducing the development of hepatocellular carcinoma by regulating miRNA activity. *FASEB J.* [Epub ahead of print] doi: 10.1096/fj.12-220905 fj.12-220905

Goljanek-Whysall, K., Pais, H., Rathjen, T., Sweetman, D., Dalmay, T. and Münsterberg, A. (2012). Regulation of multiple target genes by miR-1 and miR-206 is pivotal for C2C12 myoblast differentiation. *J. Cell Sci.* **125**, 3590-3600.

Gong, M., Meng, L., Jiang, B., Zhang, J., Yang, H., Wu, J. and Shou, C. (2008). p37 from Mycoplasma hyorhinis promotes cancer cell invasiveness and metastasis through activation of MMP-2 and followed by phosphorylation of EGFR. *Mol. Cancer Ther.* **7**, 530-537.

Huang, Q., Gumireddy, K., Schrier, M., le Sage, C., Nagel, R., Nair, S., Egan, D. A., Li, A., Huang, G., Klein-Szanto, A. J. et al. (2008). The microRNAs miR-373 and miR-520c promote tumour invasion and metastasis. *Nat. Cell Biol.* **10**, 202-210.

Huynh, H., Bottini, N., Williams, S., Cherepanov, V., Musumeci, L., Saito, K., Bruckner, S., Vachon, E., Wang, X., Kruger, J. et al. (2004). Control of vesicle fusion by a tyrosine phosphatase. *Nat. Cell Biol.* **6**, 831-839.

Jeyapalan, Z., Deng, Z., Shatseva, T., Fang, L., He, C. and Yang, B. B. (2011). Expression of CD44 3′-untranslated region regulates endogenous microRNA functions in tumorigenesis and angiogenesis. *Nucleic Acids Res.* **39**, 3026-3041.

Kahai, S., Lee, S. C., Lee, D. Y., Yang, J., Li, M., Wang, C. H., Jiang, Z., Zhang, Y., Peng, C. and Yang, B. B. (2009). MicroRNA miR-378 regulates nephronectin expression modulating osteoblast differentiation by targeting GalNT-7. *PLoS ONE* **4**, e7535.

Koletsa, T., Kotoula, V., Karayannopoulou, G., Nenopoulou, E., Karkavelas, G., Papadimitriou, C. S. and Kostopoulos, I. (2010). EGFR expression and activation are common in HER2 positive and triple-negative breast tumours. *Histol. Histopathol.* **25**, 1171-1179.

Lagos-Quintana, M., Rauhut, R., Lendeckel, W. and Tuschl, T. (2001). Identification of novel genes coding for small expressed RNAs. *Science* **294**, 853-858.

Lal, A., Kim, H. H., Abdelmohsen, K., Kuwano, Y., Pullmann, R., Jr., Srikantan, S., Subrahmanyam, R., Martindale, J. L., Yang, X., Ahmed, F. et al. (2008). p16(INK4a) translation suppressed by miR-24. *PLoS ONE* **3**, e1864. doi:10.1371/journal.pone.0001864

Lal, A., Navarro, F., Maher, C. A., Maliszewski, L. E., Yan, N., O'Day, E., Chowdhury, D., Dykxhoorn, D. M., Tsai, P., Hofmann, O. et al. (2009). miR-24 Inhibits cell proliferation by targeting E2F2, MYC, and other cell-cycle genes via binding to "seedless" 3'UTR microRNA recognition elements. *Mol. Cell* **35**, 610-625.

LaPierre, D. P., Lee, D. Y., Li, S. Z., Xie, Y. Z., Zhong, L., Sheng, W., Deng, Z. and Yang, B. B. (2007). The ability of versican to simultaneously cause apoptotic resistance and sensitivity. *Cancer Res.* **67**, 4742-4750.

Lee, D. Y., Deng, Z., Wang, C. H. and Yang, B. B. (2007). MicroRNA-378 promotes cell survival, tumor growth, and angiogenesis by targeting SuFu and Fus-1 expression. *Proc. Natl. Acad. Sci. USA* **104**, 20350-20355.

Lee, D. Y., Shatseva, T., Jeyapalan, Z., Du, W. W., Deng, Z. and Yang, B. B. (2009). A 3′-untranslated region (3'UTR) induces organ adhesion by regulating miR-199a* functions. *PLoS ONE* **4**, e4527.

Lin, S. C., Liu, C. J., Lin, J. A., Chiang, W. F., Hung, P. S. and Chang, K. W. (2010). miR-24 up-regulation in oral carcinoma: positive association from clinical and in vitro analysis. *Oral Oncol.* **46**, 204-208.

Luo, L., Ye, G., Nadeem, L., Fu, G., Yang, B. B., Honarparvar, E., Dunk, C., Lye, S. and Peng, C. (2012). MicroRNA-378a-5p promotes trophoblast cell survival, migration and invasion by targeting Nodal. *J. Cell Sci.* **125**, 3124-3132.

Lynch, T. J., Bell, D. W., Sordella, R., Gurubhagavatula, S., Okimoto, R. A., Brannigan, B. W., Harris, P. L., Haserlat, S. M., Supko, J. G., Haluska, F. G. et al. (2004). Activating mutations in the epidermal growth factor receptor underlying responsiveness of non-small-cell lung cancer to gefitinib. *N. Engl. J. Med.* **350**, 2129-2139.

Ma, L., Teruya-Feldstein, J. and Weinberg, R. A. (2007). Tumour invasion and metastasis initiated by microRNA-10b in breast cancer. *Nature* **449**, 682-688.

Magkou, C., Nakopoulou, L., Zoubouli, C., Karali, K., Theohari, I., Bakarakos, P. and Giannopoulou, I. (2008). Expression of the epidermal growth factor receptor (EGFR) and the phosphorylated EGFR in invasive breast carcinomas. *Breast Cancer Res.* **10**, R49.

Naundorf, H., Rewasowa, E. C., Fichtner, I., Büttner, B., Becker, M. and Görlich, M. (1992). Characterization of two human mammary carcinomas, MT-1 and MT-3, suitable for in vivo testing of ether lipids and their derivatives. *Breast Cancer Res. Treat.* **23**, 87-95.

Nohata, N., Hanazawa, T., Enokida, H. and Seki, N. (2012). microRNA-1/133a and microRNA-206/133b clusters: dysregulation and functional roles in human cancers. *Oncotarget* **3**, 9-21.

Qian, L., Van Laake, L. W., Huang, Y., Liu, S., Wendland, M. F. and Srivastava, D. (2011). miR-24 inhibits apoptosis and represses Bim in mouse cardiomyocytes. *J. Exp. Med.* **208**, 549-560.

Qin, W., Shi, Y., Zhao, B., Yao, C., Jin, L., Ma, J. and Jin, Y. (2010). miR-24 regulates apoptosis by targeting the open reading frame (ORF) region of FAF1 in cancer cells. *PLoS ONE* **5**, e9429.

Rutnam, Z. J. and Yang, B. B. (2012a). The involvement of microRNAs in malignant transformation. *Histol. Histopathol.* **27**, 1263-1270.

Rutnam, Z. J. and Yang, B. B. (2012b). The non-coding 3′ UTR of CD44 induces metastasis by regulating extracellular matrix functions. *J. Cell Sci.* **125**, 2075-2085.

Schmidt-Ullrich, R. K., Mikkelsen, R. B., Dent, P., Todd, D. G., Valerie, K., Kavanagh, B. D., Contessa, J. N., Rorrer, W. K. and Chen, P. B. (1997). Radiation-induced proliferation of the human A431 squamous carcinoma cells is dependent on EGFR tyrosine phosphorylation. *Oncogene* **15**, 1191-1197.

Seitz, H., Youngson, N., Lin, S. P., Dalbert, S., Paulsen, M., Bachellerie, J. P., Ferguson-Smith, A. C. and Cavaillé, J. (2003). Imprinted microRNA genes transcribed antisense to a reciprocally imprinted retrotransposon-like gene. *Nat. Genet.* **34**, 261-262.

Shan, S. W., Lee, D. Y., Deng, Z., Shatseva, T., Jeyapalan, Z., Du, W. W., Zhang, Y., Xuan, J. W., Yee, S. P., Siragam, V. et al. (2009). MicroRNA MiR-17 retards tissue growth and represses fibronectin expression. *Nat. Cell Biol.* **11**, 1031-1038.

Shan, S. W., Fang, L., Shatseva, T., Rutnam, Z. J., Yang, X., Du, W. W., Lu, W.-Y., Xuan, J. W., Deng, Z. and Yang, B. B. (2013). Mature miR-17-5p and passenger miR-17-3p induce hepatocellular carcinoma by targeting PTEN, GalNT7 and vimentin in different signal pathways. *J. Cell Sci.* **126**, 1517-1530.

Shatseva, T., Lee, D. Y., Deng, Z. and Yang, B. B. (2011). MicroRNA miR-199a-3p regulates cell proliferation and survival by targeting caveolin-2. *J. Cell Sci.* **124**, 2826-2836.

Siragam, V., Rutnam, Z. J., Yang, W., Fang, L., Luo, L., Yang, X., Li, M., Deng, Z., Qian, J., Peng, C. et al. (2012). MicroRNA miR-98 inhibits tumor angiogenesis and invasion by targeting activin receptor-like kinase-4 and matrix metalloproteinase-11. *Oncotarget* **3**, 1370-1385.

Smits, M., Nilsson, J., Mir, S. E., van der Stoop, P. M., Hulleman, E., Niers, J. M., de Witt Hamer, P. C., Marquez, V. E., Cloos, J., Krichevsky, A. M. et al. (2010). miR-101 is down-regulated in glioblastoma resulting in EZH2-induced proliferation, migration, and angiogenesis. *Oncotarget* **1**, 710-720.

Song, L. and Tuan, R. S. (2006). MicroRNAs and cell differentiation in mammalian development. *Birth Defects Res. C Embryo Today* **78**, 140-149.

Sørensen, O. E., Thapa, D. R., Roupé, K. M., Valore, E. V., Sjöbring, U., Roberts, A. A., Schmidtchen, A. and Ganz, T. (2006). Injury-induced innate immune response in human skin mediated by transactivation of the epidermal growth factor receptor. *J. Clin. Invest.* **116**, 1878-1885.

Swanton, C., Szallasi, Z., Brenton, J. D. and Downward, J. (2008). Functional genomic analysis of drug sensitivity pathways to guide adjuvant strategies in breast cancer. *Breast Cancer Res.* **10**, 214.

Tonks, N. K. (2006). Protein tyrosine phosphatases: from genes, to function, to disease. *Nat. Rev. Mol. Cell Biol.* **7**, 833-846.

Viticchiè, G., Lena, A. M., Latina, A., Formosa, A., Gregersen, L. H., Lund, A. H., Bernardini, S., Mauriello, A., Miano, R., Spagnoli, L. G. et al. (2011). MiR-203 controls proliferation, migration and invasive potential of prostate cancer cell lines. *Cell Cycle* **10**, 1121-1131.

Volinia, S., Calin, G. A., Liu, C. G., Ambs, S., Cimmino, A., Petrocca, F., Visone, R., Iorio, M., Roldo, C., Ferracin, M. et al. (2006). A microRNA expression signature of human solid tumors defines cancer gene targets. *Proc. Natl. Acad. Sci. USA* **103**, 2257-2261.

Walker, F., Abramowitz, L., Benabderrahmane, D., Duval, X., Descatoire, V., Hénin, D., Lehy, T. and Aparicio, T. (2009). Growth factor receptor expression in anal squamous lesions: modifications associated with oncogenic human papillomavirus and human immunodeficiency virus. *Hum. Pathol.* **40**, 1517-1527.

Wang, C. H., Lee, D. Y., Deng, Z., Jeyapalan, Z., Lee, S. C., Kahai, S., Lu, W. Y., Zhang, Y. and Yang, B. B. (2008a). MicroRNA miR-328 regulates zonation morphogenesis by targeting CD44 expression. *PLoS ONE* **3**, e2420.

Wang, X., Tang, S., Le, S. Y., Lu, R., Rader, J. S., Meyers, C. and Zheng, Z. M. (2008b). Aberrant expression of oncogenic and tumor-suppressive microRNAs in cervical cancer is required for cancer cell growth. *PLoS ONE* **3**, e2557.

Xie, L., Wang, T., Yu, S., Chen, X., Wang, L., Qian, X., Yu, L., Ding, Y., Zhang, C. and Liu, B. (2011). Cell-free miR-24 and miR-30d, potential diagnostic biomarkers in malignant effusions. *Clin. Biochem.* **44**, 216-220.

Yang, X., Rutnam, Z. J., Jiao, C., Wei, D., Xie, Y., Du, J., Zhong, L. and Yang, B. B. (2012). An anti-let-7 sponge decoys and decays endogenous let-7 functions. *Cell Cycle* **11**, 3097-3108.

Ye, G., Fu, G., Cui, S., Zhao, S., Bernaudo, S., Bai, Y., Ding, Y., Zhang, Y., Yang, B. B. and Peng, C. (2011). MicroRNA 376c enhances ovarian cancer cell survival by targeting activin receptor-like kinase 7: implications for chemoresistance. *J. Cell Sci.* **124**, 359-368.

Yu, B., Zhou, S., Wang, Y., Qian, T., Ding, G., Ding, F. and Gu, X. (2012). miR-221 and miR-222 promote Schwann cell proliferation and migration by targeting LASS2 after sciatic nerve injury. *J. Cell Sci.* **125**, 2675-2683.

Yuan, T., Wang, Y., Zhao, Z. J. and Gu, H. (2010). Protein-tyrosine phosphatase PTPN9 negatively regulates ErbB2 and epidermal growth factor receptor signaling in breast cancer cells. *J. Biol. Chem.* **285**, 14861-14870.

Zaidi, S. K., Dowdy, C. R., van Wijnen, A. J., Lian, J. B., Raza, A., Stein, J. L., Croce, C. M. and Stein, G. S. (2009). Altered Runx1 subnuclear targeting enhances myeloid cell proliferation and blocks differentiation by activating a miR-24/MKP-7/MAPK network. *Cancer Res.* **69**, 8249-8255.

Zhang, H., Berezov, A., Wang, Q., Zhang, G., Drebin, J., Murali, R. and Greene, M. I. (2007). ErbB receptors: from oncogenes to targeted cancer therapies. *J. Clin. Invest.* **117**, 2051-2058.

Zhu, J. H., Chen, R., Yi, W., Cantin, G. T., Fearns, C., Yang, Y., Yates, J. R., 3rd and Lee, J. D. (2008). Protein tyrosine phosphatase PTPN13 negatively regulates Her2/ErbB2 malignant signaling. *Oncogene* **27**, 2525-2531.

Zou, C., Xu, Q., Mao, F., Li, D., Bian, C., Liu, L. Z., Jiang, Y., Chen, X., Qi, Y., Zhang, X. et al. (2012). MiR-145 inhibits tumor angiogenesis and growth by N-RAS and VEGF. *Cell Cycle* **11**, 2137-2145.

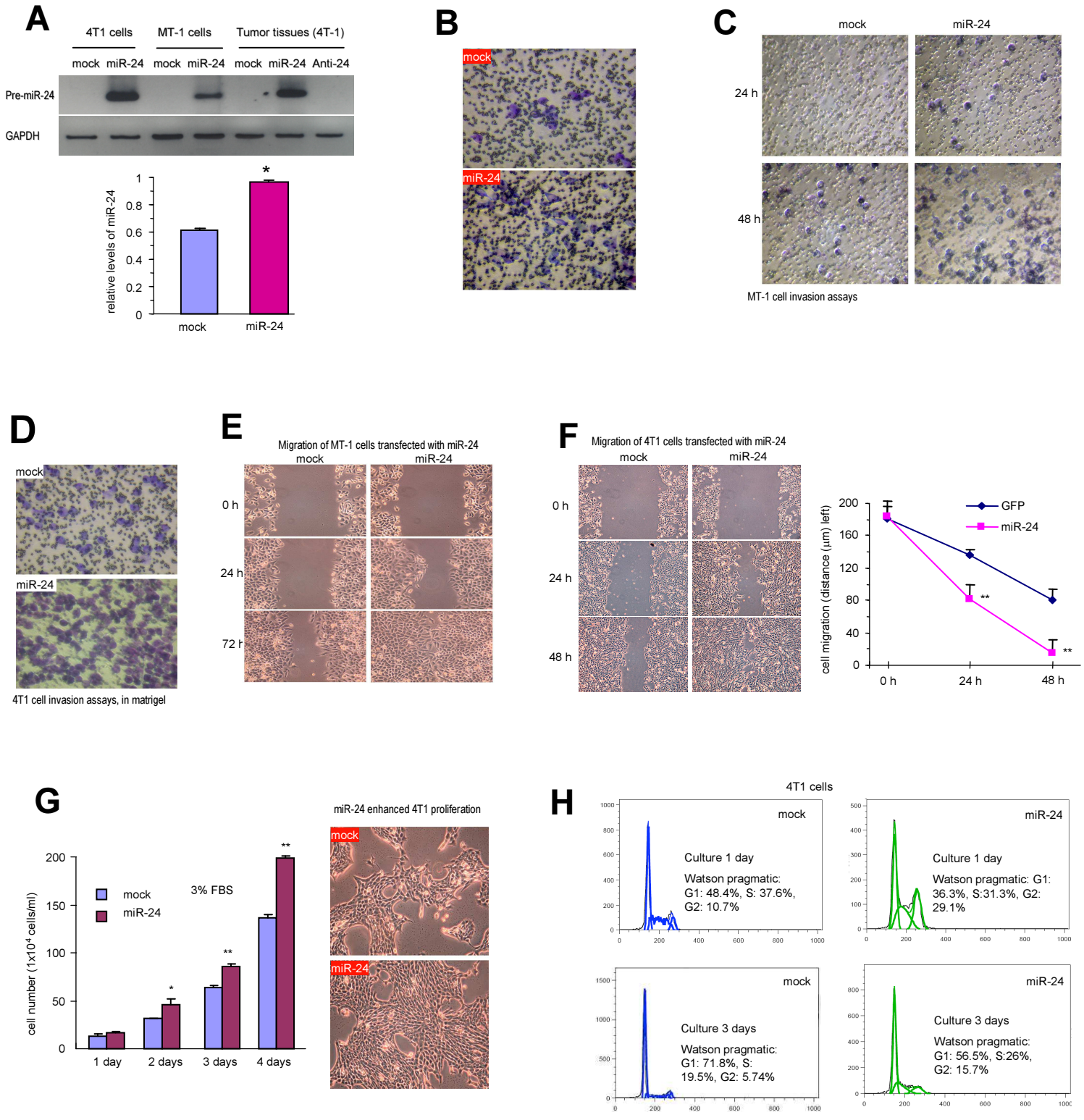

Fig S1. Expression of miR-24 enhanced breast cancer cell invasion, migration and proliferation. (**A**) Upper, DNAs isolated from 4T1 cells, MT-1 cells, and tumors expressing miR-24, anti-miR-24, or mock were subjected to PCR to confirm integration of miR-24 into the genome. Lower, RNAs were isolated from mock and miR-24 transiently transfected 4T1 cells and subjected to real-time PCR to measure mature miR-24 levels. Asterisks indicate significant differences. * $p<0.05$. Error bars, SD (n=3). (**B**) Mock- and miR-24-transfected 4T1 cells ($1x10^5$) were loaded into the insert with 100 ml serum-free DMEM medium and then incubated at 37° C for 12 hours. The migrated cells were stained blue and were counted in 6 randomly selected fields under a light microscope. (**C**) Mock- and miR-24-transfected MT-1 cells ($1x10^5$) suspended in 100 ml serum-free medium were loaded in the transwell insert containing Matrigel and incubated at 37° C for 24 hours for cell invasion assays. Expression of miR-24 promoted invasion. (**D**) Mock- and miR-24-transfected 4T1 cells ($1x10^5$) were subject to the same invasion assays. (**E**) Mock- and miR-24-transfected MT-1 cultures were wounded with a 200-μl pipette tip and cultured in 10% FBS/DMEM medium with 2 μM mytomycin for cell migration assay. Expression of miR-24 promoted migration. (**F**) Mock- and miR-24-transfected 4T1 cultures were subject to the same migration assay. (**G**) 4T1 cells stably transfected with miR-24 or mock were maintained in tissue culture dishes in DMEM with 3% FBS. Cell proliferation was determined by cell counting. **, $p< 0.01$, n=6. Right, typical photos of proliferating cells. (**H**) Mock- and miR-24transfected 4T1 cells ($5x10^5$) were analyzed for cell cycle progression. Fewer miR-24 cells were present in G1 phase than mock cells.

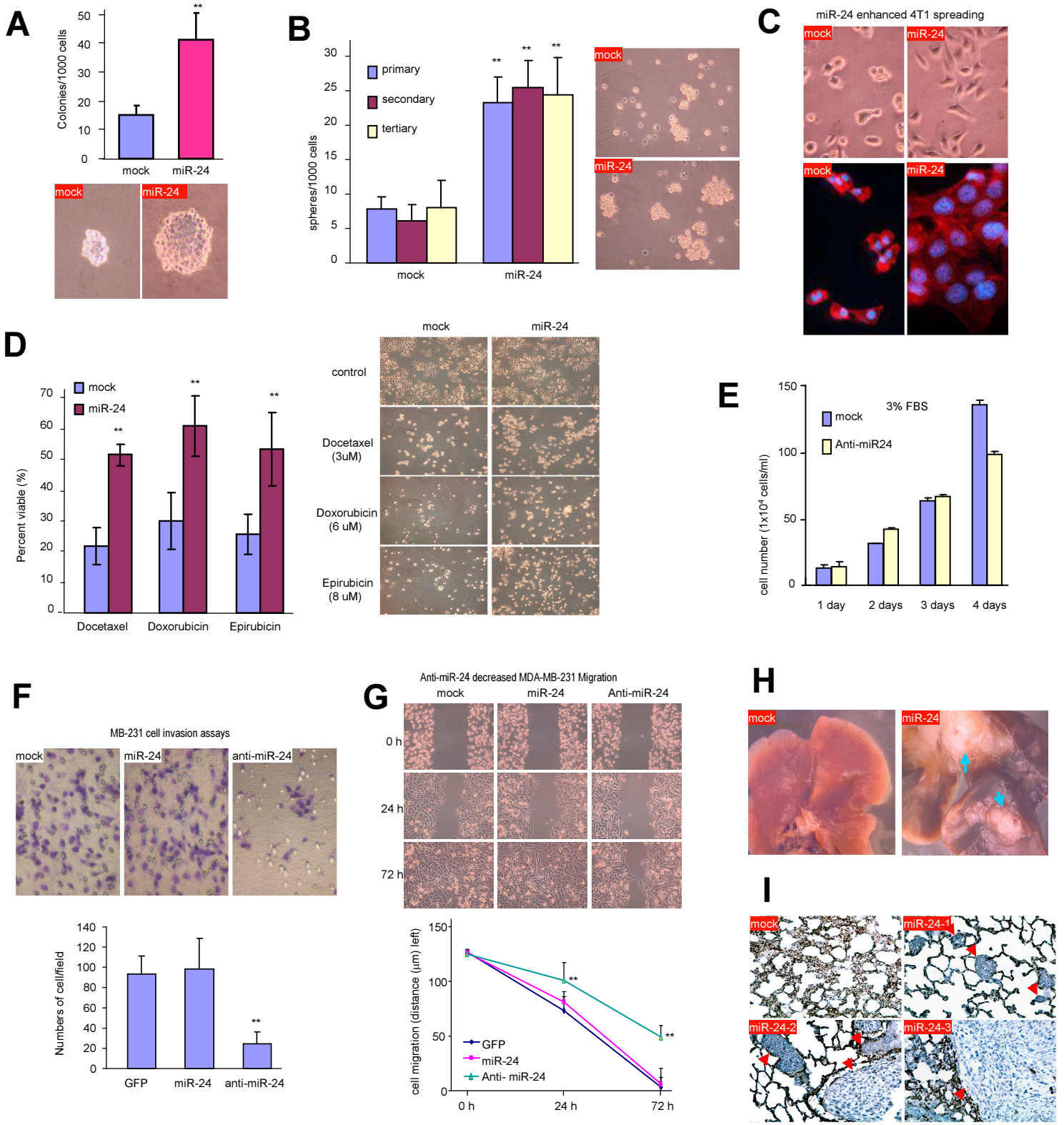

Fig S2. Expression of miR-24 enhanced colony formation, sphere formation, cell spreading, drug resistance, tumor invasion, and metastasis. (**A**) Mock- and miR-24-transfected MT-1 cells (103) were subject to colony formation assay. The number of colonies was counted in 6 fields of views for each plate. **, $p< 0.01$, $n = 6$. Lower, typical photos of colonies. (**B**) Mock- and miR-24-transfected MT-1 cells were subject to mammosphere formation assay. The numbers of mammospheres were counted in 6 randomly selected fields. **, $p< 0.01$, $n = 6$. Right, typical mammospheres after cultured in Petri dishes for 10 days. (**C**) 4T1 cells transfected with miR-24 or mock were maintained in tissue culture dishes in DMEM containing 3% FBS. Cell morphology was monitored with a light microscope (upper) or examined after immunostaining (lower) to detect actin filaments (red) and nuclei (blue). (**D**) Mock- and miR-24-transfected MT-1 cells ($1x10^4$ cells/well) were inoculated and cultured in 10% FBS/DMEM medium in 96-well culture dishes for 12 hours. After cell attachment, the medium was changed to 10% FBS/DMEM containing 3 μM Docetaxel, 6 μM Doxoeubicin or 8 μM Epirubicin for 24 hours. The cultures were incubated with 10 μl WST-1 reagent for 4 hours. The absorbance of the samples against a background blank control was measured by a microplate reader. **, $p< 0.01$, n=9. Expression of miR-24 led to acquired drug-resistance of the cells. Right, typical photos are shown. (**E**) Mock- and anti-miR-24-transfected 4T1 cells were subject to proliferation assay in DMEM supplemented with 3% FBS ($n = 6$). (**F**) Mock-, miR-24-, and anti-miR-24-transfected MDA-MB-231 cells (1x105) were subjected to invasion assays for 48 hours. miR-24 enhanced cell invasion but anti-miR-24 inhibited it. The invasive cells were counted for statistical analysis (lower). (**G**) Mock-, miR-24-, and anti-miR-24-transfected MDA-MB-231 cultures were subject to migration assays. Transfection with anti-miR-24 decreased cell migration. The migration distance was measured for statistical analysis (lower). (**H**) Mock- and miR-24-transfected MT-1 cells ($2×10^5$) were injected into NOD-SCID mice via tail vein, with 15 mice in each group. Six weeks after the injection, 3 mice in the miR-24 group developed cachexia, and 4 had lung metastasis in necroscopy. Typical metastatic lesions in the lungs are shown (arrows). (**I**) H&E staining of lungs from mock and miR-24 lung showed multi-focal metastasis lesions in the miR-24 lungs (arrows).

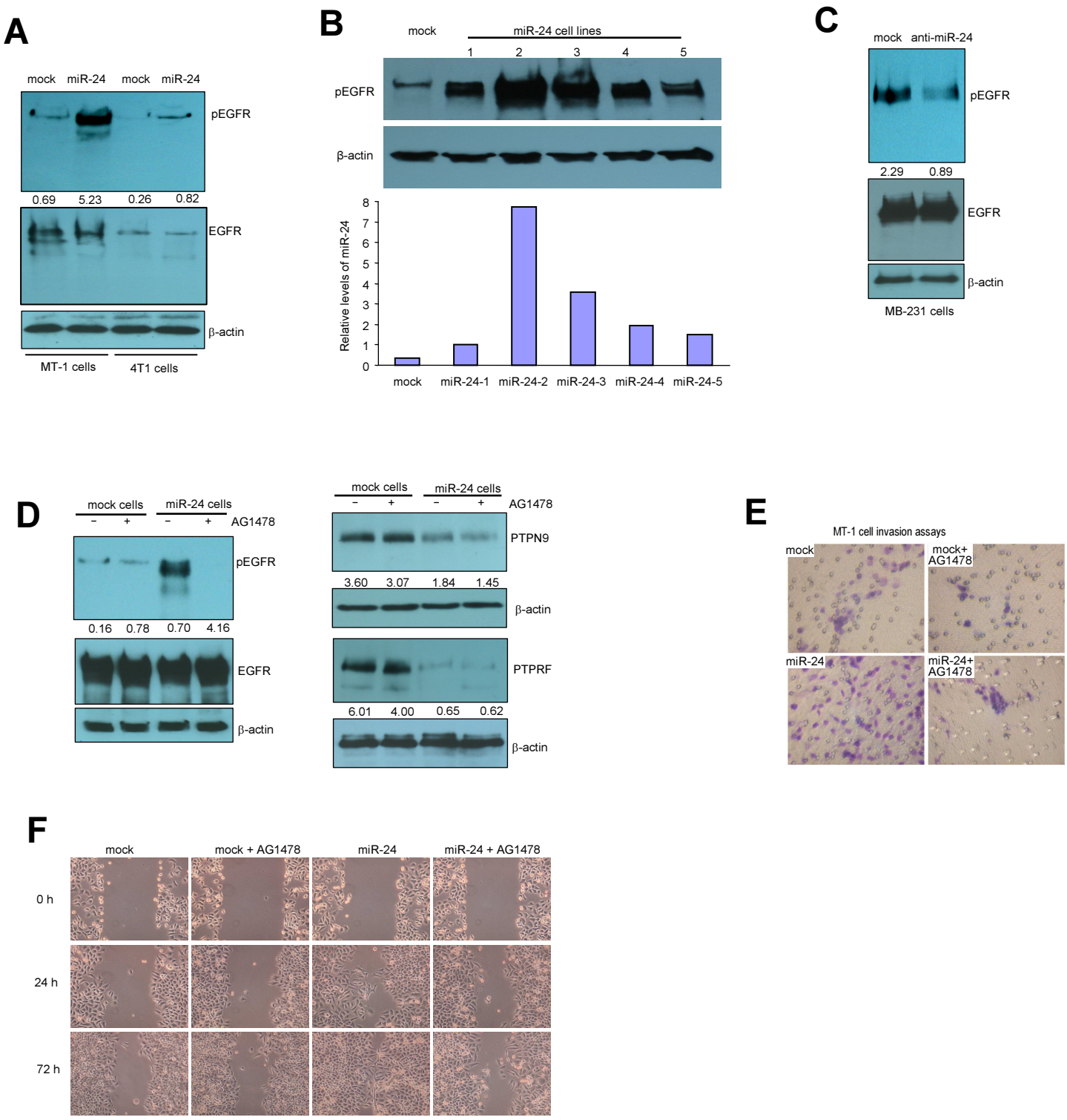

Fig S3. miR-24 affect pEGFR expression and functions. (**A**) Cell lysates from mock- and miR-24-transfected 4T1 and MT-1 cells were analyzed on Western blotting for levels of pEGFR, EGFR and b-actin. Expression of miR-24 increased pEGFR levels. (**A**) Single cell suspensions were plated on 96 well culture dishes. After culturing for an additional 2 days, single colony cells were moved to 6-well dishes and cultured to 70 % conference. Cell lysates were prepared and subjected to Western blot analysis for pEGFR expression. Higher levels of miR-24 were associated with higher levels of pEGFR. (**C**) Cell lysates prepared from vector- and anti-miR-24-transfected MDA-MB-231 cells were subjected to immunoblotting probed with antibodies against pEGFR, EGFR and b-actin. (**D**) Left, cell lysates prepared from mock- and miR-24-transfected MT-1 cells pre-treated with 2.0 μM AG 1478 for 24 hours were subjected to immunoblotting probed with antibodies against pEGFR, EGFR and b-actin. Increased levels of pEGFR by miR-24 expression was abolished by AG1478 treatment. Right, the lysates were also subjected to Western blot analysis for expression of PTPN9 and PTPRF. Treatment with AG1478 had little effect on expression of PTPN9 and PTPRF. (**E**) Mock- and miR-24-transfected MT-1 cells ($1x10^5$) were subject to invasion assays with or without 2.0 μM AG1478 treatment for 56 hours. The increased invasion due to miR-24 expression was abolished by AG1478 treatment. (**F**) Mock- and miR-24-transfected MT-1 cultures were treated with or without 2.0 μM AG1478 for migration assay. Increased cell migration acquired by miR-24 expression was abolished by AG1478 treatment.

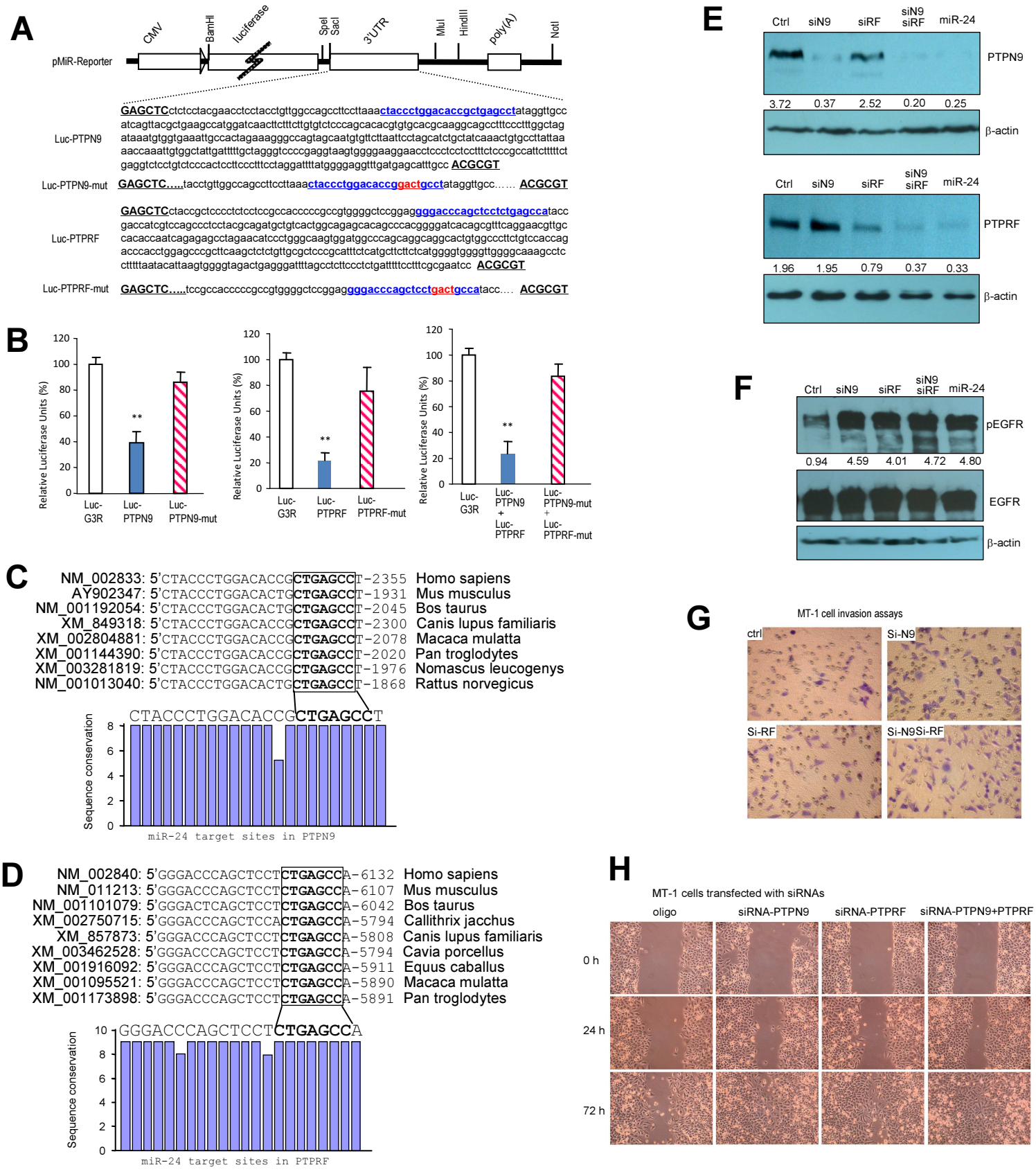

Fig S4. miR-24 targeting analyses. (**A**) Fragments of PTPN9 and PTPRF 3'UTRs were inserted into the luciferase report vector pMir-Report producing constructs Luc-PTPN9 and Luc-PTPRF. The potential miR-24 target sites were labeled in blue. Mutations labeled in red were generated in the miR-24 target sites producing mutant constructs Luc-PTPN9-mut and Luc-PTPN9-mut. (**B**) U343 cells were co-transfected with miR-24 and a luciferase reporter construct, as shown in the figure, for luciferase assays. Presence of the miR-24 target site reduced luciferase activities, which were reversed when the target site was mutated (n=9). (**C**) Alignment of the miR-24 target sites in PTPN9 across different species as shown. The miR-24/PTPN9 target sites are bolded. Conservation of the sequences is shown across all species. (**D**) Alignment of the miR-24 target sites in PTPRF across different species. The miR-24/PTPRF target sites are bolded. (**E**) Cell lysates prepared from MT-1 cells transfected with siRNAs against PTPN9 (siN9) and PTPRF (siRF) were subjected to Western blot analysis to confirm silencing of PTPN9 and PTPRF. (**F**) Treatment with 20 ng/ml EGF enhanced EGFR phospharylation, which had additive effect with PTPN9 and PTPEF silencing. (**G**) MT-1 cells (1x10^5) transfected with control oligo, siRNAs against PTPN9 and PTPRF as indicated were incubated at 37° C for 64 hours for invasion assays. Transfection with siN9 and siRF promoted cell invasion. (**H**) MT-1 cells (4x10^5) transfected with control oligo, siN9, and siRF were subject to migration assays. Transfection with siN9 and siRF promoted migration.

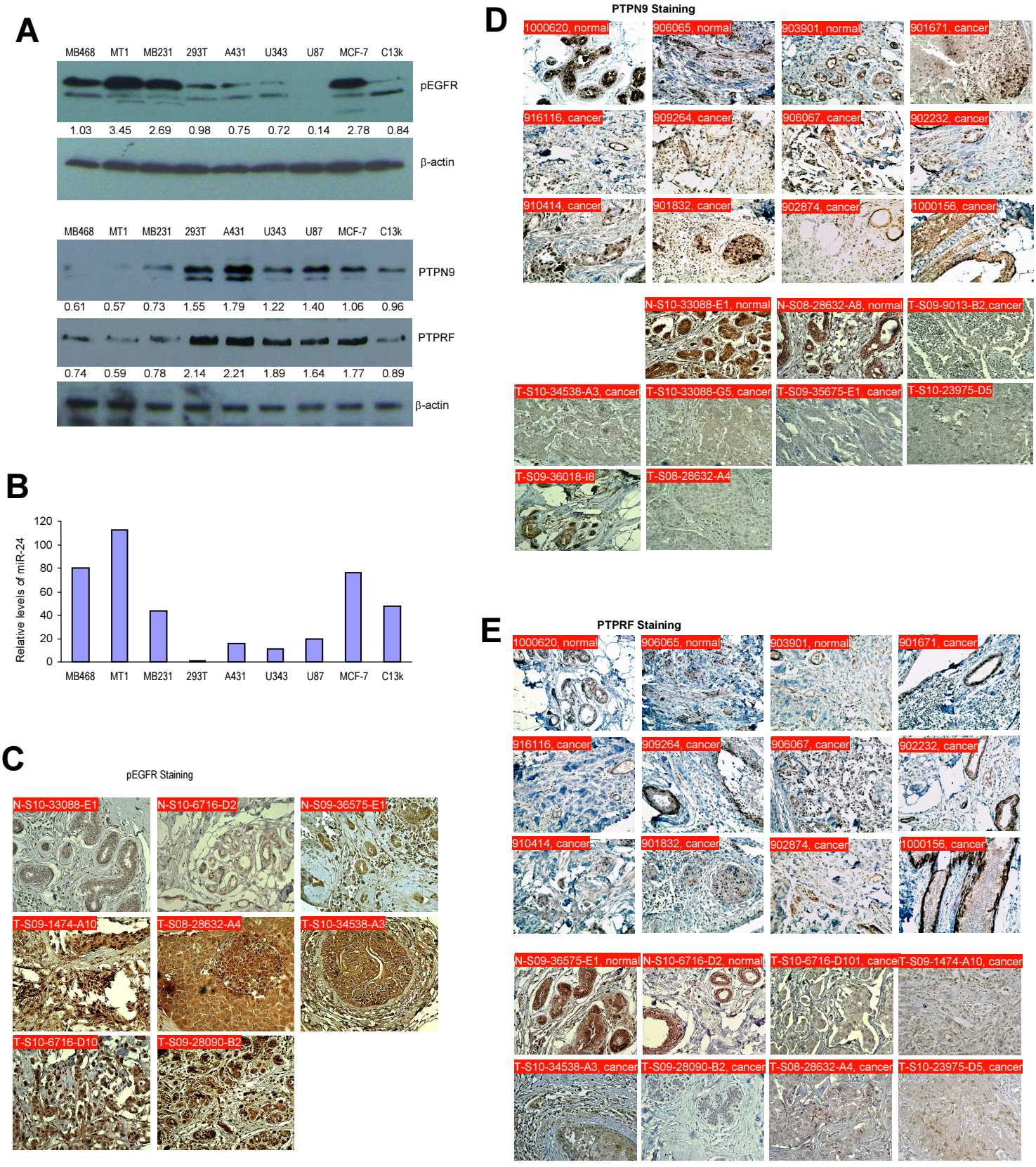

Fig S5. Relationship of the expression of pEGFR, PTPN9, PTPRF, and miR-24. (**A**) Cell lysates prepared from different cell lines were subjected to western blot analysis probed with anti-pEGFR, PTPN9, and PTPRF antibodies. While expression of pEGFR was high in the human breast cancer cell lines MB-468, MT-1, and MB-231, expression of PTPN9 and PTPRF was relatively low in these three cell lines. (**B**) Expression of miR-24 was analyzed on these cell lines with real-time PCR. The levels of miR-24 were relatively high in the three cell lines indicated above. (**C**) Human breast cancer tumors and normal breast tissues from The Affiliated People's Hospital of Jiangsu University were sectioned, and stained with antibody against pEGFR. Increased staining was detected in the tumor tissues. (**D**) Human breast cancer tumors and normal breast tissues obtained from (upper) The Affiliated People's Hospital of Jiangsu University and (lower) University of Iowa Carver College of Medicine were sectioned, and stained with antibody against PTPN9. Decreased staining was detected in the tumor tissues. (**E**) Human breast cancer tumors and normal breast tissues obtained from (upper) The Affiliated People's Hospital of Jiangsu University and (lower) University of Iowa Carver College of Medicine were sectioned, and stained with antibody against PTPRF. Decreased staining was detected in the tumor tissues.

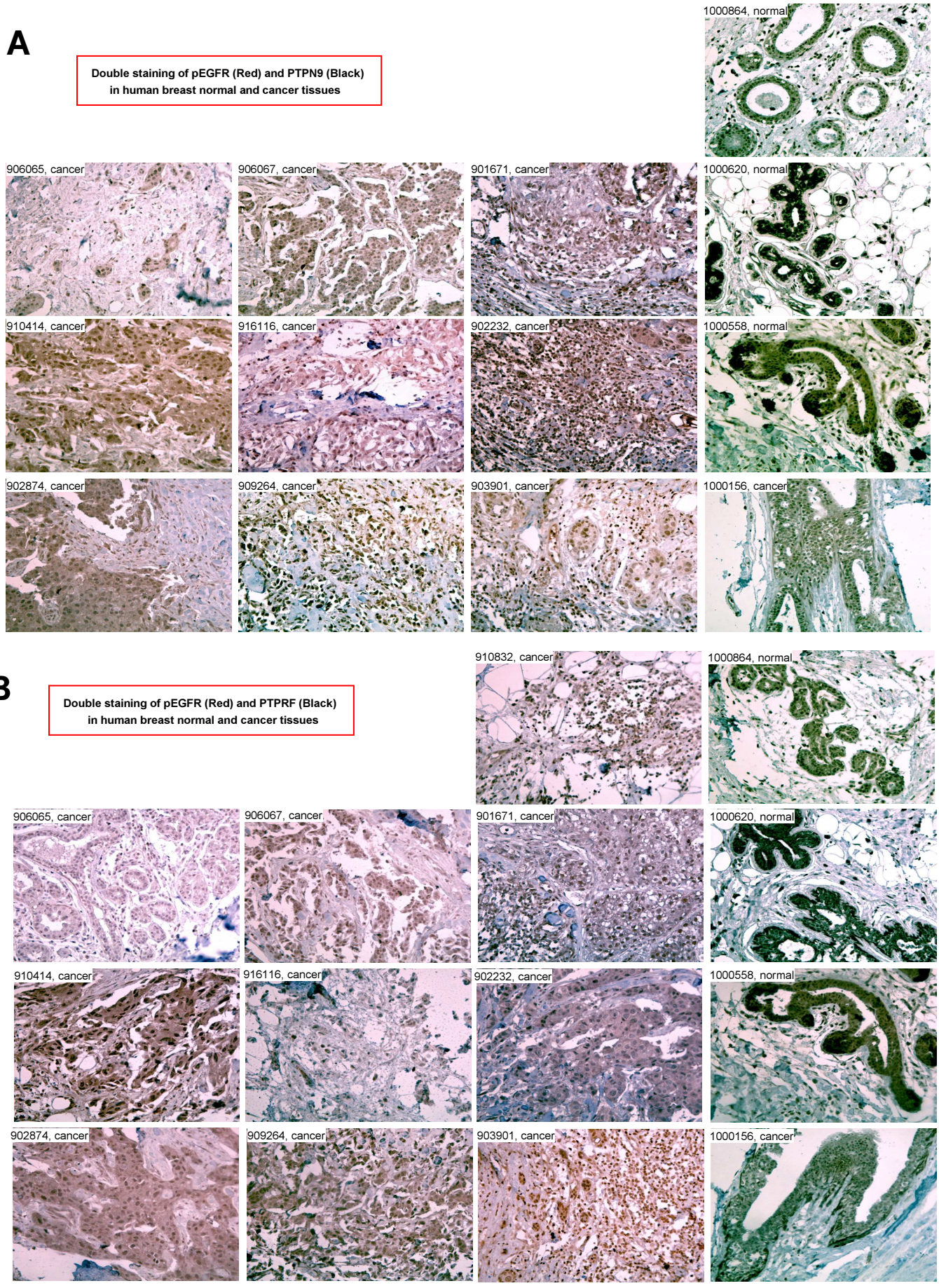

Fig S6. Double staining of pEGFR with PTPN9 or PTPRF. (**A**) Human breast cancer tumors and normal breast tissues were sectioned, and incubated with antibody to pEGFR, and stained with ACE (Red, SK-4200). After blocking with avidin/biotin blocking kit (SP-2001), all samples were incubated with antibody to PTPN9, and then stained with DAB (Black, SK-4100). (**B**) The sections were also double stained with anti-pEGFR antibody (Red) and anti-PTPRF (Black) antibodies.

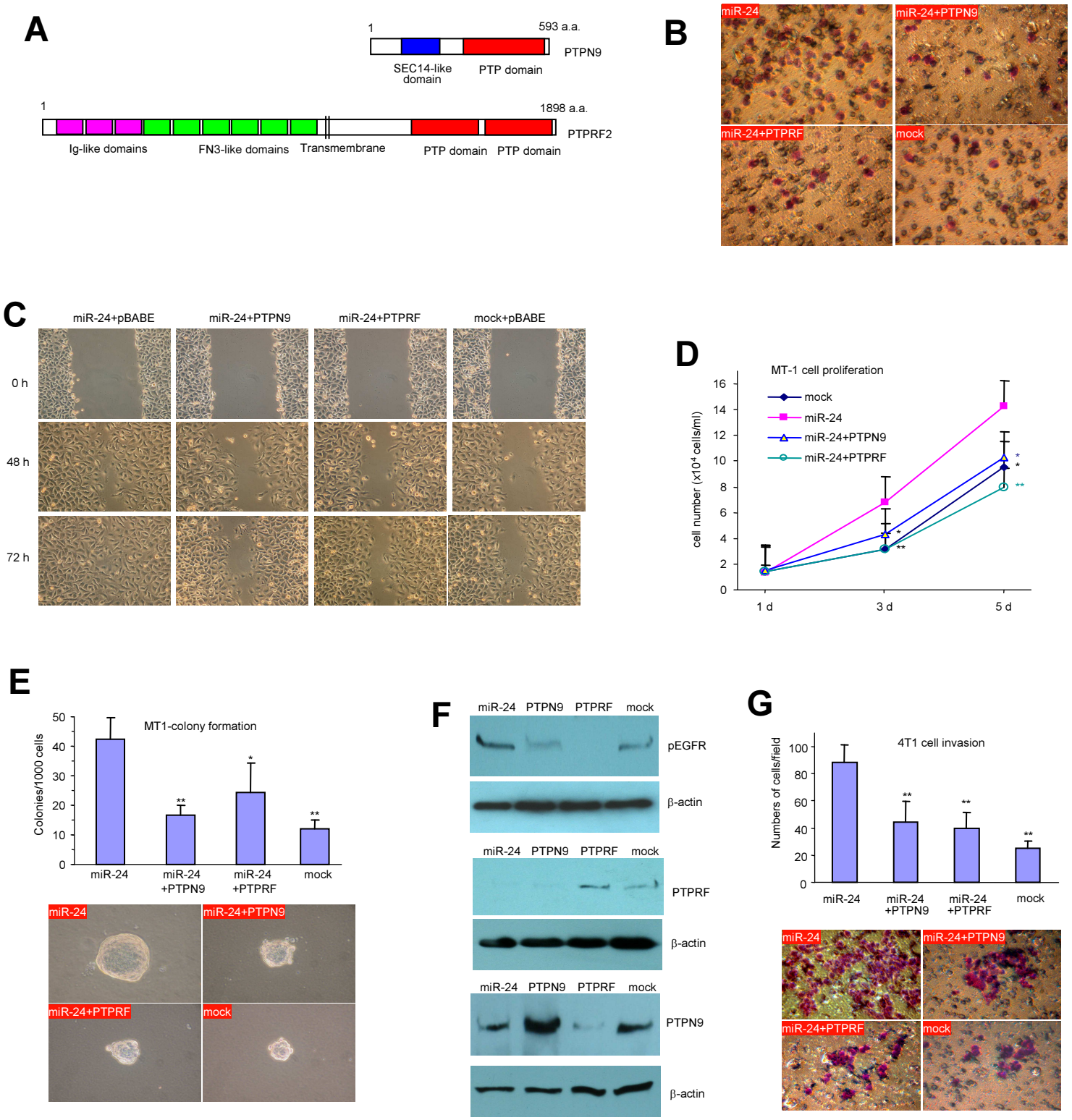

Fig S7. Reversed effects of PTPN9 and PTPRF on cell activities. (**A**) Constructs of PTPN9 and PTPRF. (**B**) Mock-, miR-24-, miR-24 and PTPN9-, or miR-24 and PTPRF-transfected MT-1 cells ($1x10^5$) were incubated at 37° C for 48 hours for invasion assays. Enhanced cell invasion by miR-24 expression was abolished by transfection with PTPN9 and PTPRF. (**C**) The cells ($1x10^3$) were also subject to migration assay. Enhanced cell migration by miR-24 expression was abolished by transfection with PTPN9 and PTPRF. (**D**) MT-1 cells transfected with mock, miR-24, miR-24 and PTPN9, or miR-24 and PTPRF were maintained in tissue culture dishes in DMEM containing 1.25% FBS for 1, 3, and 5 days for proliferation assay. Increased proliferation by miR-24 expression was abolished by transfection with PTPN9 and PTPRF. *, $p< 0.05$; **, $p< 0.01$, $n = 4$. (**E**) Mock-, miR-24-, miR-24 and PTPN9-, or miR-24 and PTPRF-transfected MT-1 cells ($1x10^3$) were subject to colony formation assays. Increases in colony formation as a result of miR-24 expression was abolished by transfection with PTPN9 and PTPRF ($n = 4$). Typical photos are shown (lower). (**F**) Cell lysates prepared from 4T1 cells transfected with mock, miR-24, miR-24 and PTPN9, or miR-24 and PTPRF were subjected to Western blot analysis for expression and activation of PTPN9, PTPRF, and EGFR. Transfection with PTPN9 and PTPRF increased their expression respectively, which resulted in decrease in pEGFR levels. (**G**) The mock- and miR-24-transfected 4T1 cells ($1x10^3$) were transfected with PTPN9 and PTPRF and incubated for 48 hours for invasion assays. PTPN9 and PTPRF partially reversed the effect of miR-24 on cell invasion ($n = 8$). Lower, typical photos of cell invasion.

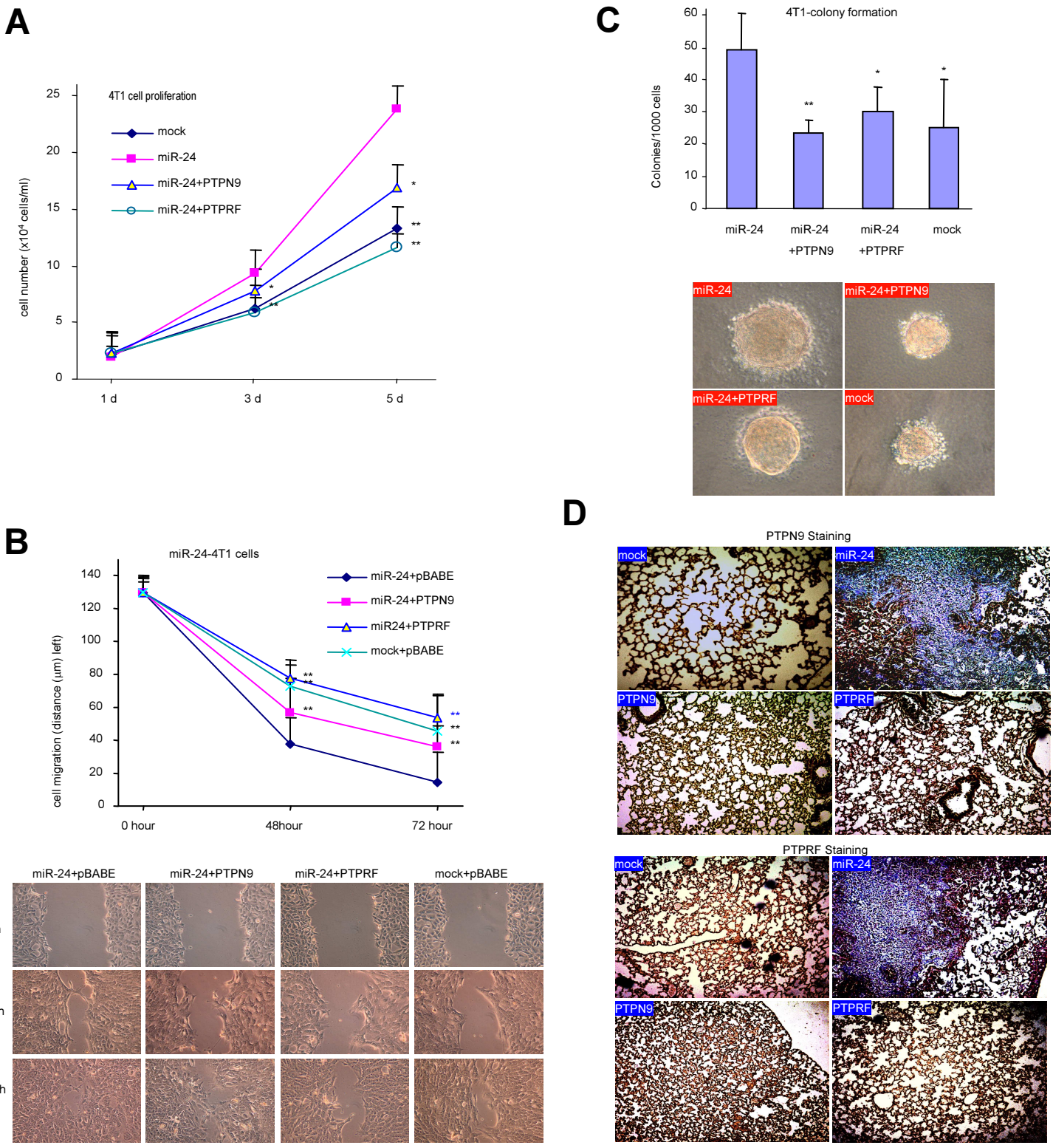

Fig S8. Reversed effects of PTPN9 and PTPRF on proliferation, migration, colony formation, and metastasis. (**A**) 4T1 cells transfected with mock, miR-24, miR-24 and PTPN9, or miR-24 and PTPRF were maintained in tissue culture dishes in DMEM with 1.25% FBS for proliferation assay (n=4). (**B**) The mock- and miR-24-transfected 4T1 cells ($1x10^3$) were transfected with PTPN9 and PTPRF as indicated for cell migration assays. PTPN9 and PTPRF reversed the effect of miR-24 on cell migration (n = 10). Lower, typical photos of cell migration. (**C**) The mock- and miR-24-transfected 4T1 cells ($1x10^3$) were transfected with PTPN9 and PTPRF and subject to colony formation assays. PTPN9 and PTPRF reversed the effect of miR-24 on the formation of colonies (n = 4). Right, typical photos of colonies. (**D**) The mock- and miR-24 lung tissues were subject to immuno-staining with anti-PTPN9 and anti-PTPRF antibodies. Increased expression of pEGFR and decreased expression of PTPN9 and PTPRF were detected in the tumor tissues.

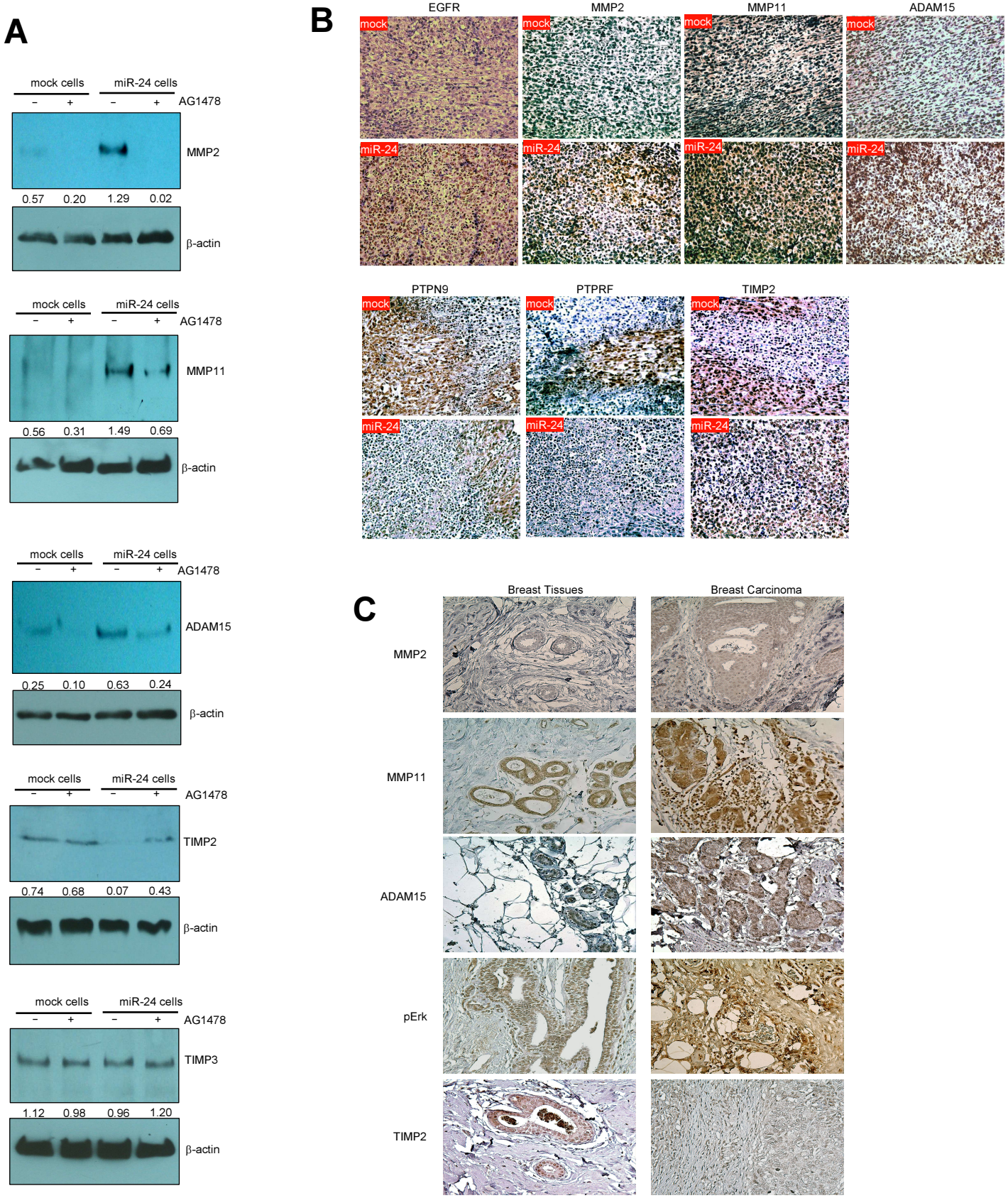

Fig S9. Effects of miR-24 on other signaling molecules. (**A**) The mock- and miR-24- transfected MT-1 cells were treated with 2.0 μM AG 1478 for 24 hours, followed by analysis on Western blot for expression of MMP2, MMP11, ADAM15, TIMP2, and TIMP3. Treatment with AG1478 down-regulated MMP2, MMP11, and ADAM15 but up-regulated TIMP2 levels in the miR-24-transfected cells. (**B**) The mock- and miR-24 tumor tissues were subjected to immunohistochemistry probed with antibodies against pEGFR, PTPN9, PTPRF, MMP2, MMP11, ADAM15, and TIMP2. Increased expression of pEGFR, MMP2, MMP11, and ADAM15 was detected, while decreased expression of PTPN9, PTPRF, and TIMP2 was detected in the tumor tissues. (**C**) Human breast carcinoma specimens were subject to immunohistochemistry probed with antibodies against MMP2, MMP11, ADAM15, pErk, and TIMP2. Increased expression of MMP2, MMP11, ADAM15, and pErk was detected, while expression of TIMP2 was decreased in the tumor tissues.

Table S1. Pathology information of patient specimens

	Age	Breast	Surgery	Histology	Grade	Tumor size	Axillary lymph nodes	ER	PR	HER2	Tumor Block	Benign Block
23975-10	27	Left	Lumpectomy	Invasive ductal carcinoma	3	3.4	Positive (1/3) Micrometastasis	Positive	Negative	Negative	D5	D8
34538-10	69	Right	Mastectomy	Invasive ductal carcinoma	2	1.5	Positive (5/10) Macrometastases	Positive	Negative	Negative	A3	A12
28090-09	33	Right	Mastectomy	Invasive ductal carcinoma	3	1.2	Positive (2/11) Macrometastases	Positive	Positive	Negative	B26	
35675-09	83	Right	Lumpectomy	Invasive ductal carcinoma	1	1.1	Positive (1/3) Macrometastases	Positive	Positive	Negative	E13	
6716-10	70	Left	Lumpectomy	Invasive ductal carcinoma	2	6.3	Positive (1/2) Macrometastases	Positive	Negative	Negative	D10	
36018-09	53	Left	Lumpectomy	Invasive ductal carcinoma	2	1.1	Positive (1/11) Macrometastases	Positive	Negative	Negative	I8	
11777-11	57	Right	Lumpectomy	Invasive ductal carcinoma	1	2.6	Positive (2/14) Macrometastases	Positive	Positive	Negative	A1	A7
33088-10	49	Right	Lumpectomy	Invasive ductal carcinoma	3	2.5	Positive (1/3) Macrometastases	Positive	Negative	Negative	G5	
28632-08	58	Left	Mastectomy	Invasive ductal carcinoma	3	4	Positive (5/12) Macrometastases	Negative	Negative	Positive	A4	A8
9013-09	45	Left	Lumpectomy	Invasive ductal carcinoma	3	1.4	Positive (1/35) Macrometastases	Negative	Negative	Negative	B26	E3
9223-10	48	Left	Lumpectomy	Invasive ductal carcinoma	2	1.1	Negative (0/2)	Positive	Positive	Negative	B2	B4
24019-10	51	Right	Mastectomy	Invasive ductal with mucinous	2	1.6	Negative (0/4)	Positive	Positive	Negative	E7	E13
21822-10	56	Left	Lumpectomy	Invasive ductal carcinoma	3	1.1	Negative (0/4)	Negative	Negative	Negative	C3	G7
28219-10	68	Left	Lumpectomy	Mucinous carcinoma	1	1.9	Negative (0/3)	Positive	Positive	Negative	C4	C6
30677-10	59	Right	Lumpectomy	Invasive ductal carcinoma	2	3.1	Negative (0/3)	Positive	Positive	Negative	C3	C8
30727-10	55	Left	Mastectomy	Invasive ductal carcinoma	3	1.9	Negative (0/4)	Negative	Negative	Negative	E4	E8
35350-10	50	Left	Lumpectomy	Invasive ductal carcinoma	3	2.6	Negative (0/1)	Positive	Positive	Positive	C3	B5
11917-11	60	Left	Lumpectomy	Invasive ductal carcinoma	2	2.9	Negative (0/2)	Positive	Positive	Negative	A1	B1
12259-11	69	Right	Lumpectomy	Invasive ductal carcinoma	1	0.4	Negative (0/4)	Positive	Positive	Negative	A18	A2
25438-10	64	Left	Mastectomy	Invasive ductal carcinoma	3	2	Negative (0/7)	Negative	Negative	Positive	D7	D19
15222-10	61	Right	Mastectomy	Invasive ductal carcinoma	2	3.8	Positive (7/14) Macrometastases	Positive	Positive	Negative	C1	D5
15195-10	65	Right	Mastectomy	Invasive ductal carcinoma	2	3.5	Positive (32/36) Macrometastases	Positive	Negative	Negative	B15	B22
21311-10	44	Left	Mastectomy	Invasive ductal carcinoma	2	2.1	Positive (1/17) Macrometastasis	Positive	Positive	Negative	A2	A1
23893-10	49	Right	Mastectomy	Invasive ductal carcinoma	2	2	Positive (1/3) Macrometastasis	Positive	Positive	Negative	D9	D12
27206-10	48	Left	Mastectomy	Invasive ductal carcinoma	2	3.1	Positive (2/12) Macrometastasis	Negative	Negative	Negative	E6	D4
27707-10	39	Right	Mastectomy	Invasive lobular carcinoma	2	0.9	Positive (1/5) Macrometastasis	Positive	Positive	Negative	B3	C8
11556-11	45	Right	Lumpectomy	Invasive ductal carcinoma	2	3.4	Positive (4/7) Macrometastases	Positive	Positive	Negative	A13	A49
1474-09	57	Left	Mastectomy	Invasive ductal carcinoma	3	2	Positive (1/11) Macrometastasis	Positive	Positive	Positive	A14	A8
25055-08	60	Left	Mastectomy	Invasive ductal carcinoma	3	0.4	Positive (12/13) Macrometastases	Negative	Negative	Positive	G2	G10
19057-08	52	Left	Mastectomy	Invasive ductal carcinoma	3	1.9	Positive (4/8) Macrometastases	Negative	Negative	Negative	B1	B16
17862-11	52	Left	Mastectomy	Invasive ductal carcinoma	3	7.8	Positive (18/18) Macrometastases	Negative	Negative	Negative	C7	
19378-11	63	Right	Mastectomy	Invasive ductal carcinoma	2	3.5	Positive (1/3) Macrometastasis	Positive	Positive	Negative	C1	
29075-11	77	Left	Mastectomy	Invasive ductal carcinoma	1	3.8	Positive (1/4) Micrometastasis	Positive	Positive	Negative	D12	
31466-11	50	Left	Mastectomy	Invasive ductal carcinoma	3	4.4	Positive (1/12) Macrometastasis	Negative	Negative	Negative	A4	
36798-11	57	Right	Lumpectomy	Invasive ductal carcinoma	3	1.7	Positive (6/19) Macrometastasis	Negative	Negative	Positive	I12	
37033-11	48	Right	Lumpectomy	Invasive ductal carcinoma	3	2.3	Positive (1/2) Macrometastasis	Negative	Negative	Negative	A5	
39338-11	42	Left	Mastectomy	Invasive ductal carcinoma	3	8	Positive (7/22) Macrometastases	Negative	Negative	Negative	A1	
20572-10	50	Left	Mastectomy	Invasive ductal carcinoma	3	6.1	Positive (2/13) Macrometastases	Negative	Negative	Negative	I4	
32212-10	57	Right	Mastectomy	Invasive ductal carcinoma	3	3.9	Positive (7/11) Macrometastases	Positive	Positive	Negative	B3	
36598-10	40	Left	Lumpectomy	Invasive ductal carcinoma	3	3.5	Positive (7/11) Macrometastases	Negative	Negative	Negative	A4	
30703-11	83	Right	Mastectomy	Invasive ductal carcinoma	1	2.5	Negative (0/3)	Positive	Positive	Negative	D6	
25800-11	74	Left	Mastectomy	Invasive ductal carcinoma	3	2.8	Negative (0/4)	Positive	Positive	Positive	D8	
19287-11	45	Right	Mastectomy	Invasive ductal carcinoma	3	3	Negative (0/2)	Positive	Positive	Positive	C2	
13853-11	66	Right	Lumpectomy	Invasive ductal carcinoma	2	2.6	Negative (0/3)	Positive	Negative	Negative	A3	
36126-10	52	Left	Mastectomy	Invasive ductal carcinoma	3	5.9	Negative (0/2)	Negative	Negative	Negative	C6	